# Beam Instrumentation in a Linear Collider

Vladimir Foguel

Doctor of Philosophy

Department of Accelerator Science
School of Mathematical and Physical Science
The Graduate University for Advanced Studies

2003

# Table of Contents

## Abstract

The design of a future multi-bunch e+e- linear collider is based on beams accelerated in very high gradient accelerator structures and having extremely small beam sizes in the collision point. For preservation of an emittance growth along the linear collider, high resolution and high accuracy BPMs are necessary. The requirements for BPMs in a LC depend on which part of LC they are installed in and do also on many other factors. In main linacs, where the number of BPMs will be around 4000, the cost of BPMs and their electronic circuits and the impedance of the BPM are most important factors. The resolution and accuracy of BPMs in this part should be comparable with the machining accuracy of accelerator structures and will be about 0.2-0.3 micrometer. It is preferable if some of these BPMs are capable of measuring the beam angle as well. For this purpose, a RF cavity BPM operated at frequency of 6,424 MHz was proposed, and calculations and experiments for study of the beam position and angle measurement resolutions were made. It was found experimentally that the cavity BPM has the beam position resolution of 180nm for both horizontal and vertical directions for a beam with electron population of $4x10^9$ to $8x10^9$ per bunch. The cavity BPM is also capable of identifying the position of each bunch in a multi-bunch train. To have the required high accelerating gradient along a linac and to produce an energy spread required by the BNS damping, we have to keep the phase between a beam and the RF accelerating voltage within an accuracy of about 1 degree. For many usages, we also need to know the bunch length distribution along a linac. This information is especially important when we first time start the beam operation. A special phase and bunch length sensor was proposed, which has combined functions of both of them in one device. Calculations and experimental results are presented.

# Chapter 1

# Introduction

# 1-1 Beam instrumentation in a Linear Collider

The design study of future high luminosity Tev e+e- Linear Colliders (LC) are presently being made by many laboratories in the world-wide collaboration. High frequency structures will be used for acceleration because reasonably high accelerating fields have been obtained by these structures, and it is possible to reduce the overall length and consequently the total cost of the linac. Two major benefits of operating at higher frequency are that (1) the stored energy required to achieve a given accelerating gradient scales as the inverse square of the frequency and (2) the breakdown field is nearly proportional to the frequency. The effective gradient in the accelerating structure for Japan Linear Collider (JLC) is 54.2MV/m at RF frequency of 11.424 GHz. To achieve the 500 Gev center-of-mass energy, it is necessary to have the linac length of about of 5.5 km for each electron and positron beam and thus the total length of linacs becomes 11 km. Another important parameter of LC is the luminosity. The luminosity of colliding beams is given by

$$L = H_D \frac{nfN^+N^-}{4\pi\sigma_x\sigma_y}, \qquad (1.1)$$

where $L$ is the luminosity, $n$ is the number of bunches, $f$ is the repetition rate, $N$+- is the number of positrons/electrons per bunch, $\sigma_x$ and $\sigma_z$ are the horizontal and vertical beam sizes in interaction point respectively, and $H_d$ is the disruption enhancement factor.

Unlike a conventional storage ring where the bunches collide many thousands of times per second, the AC and RF power sources of LC limit the repetition rate to 150 Hz. To reach high luminosity, it is necessary to collide long trains of bunches and focus them to a very small beam size at the interaction point (IP). For JLC/NLC projects, the number of bunches in one train will be 190 and the bunch spacing is 2.6 nsec. The beam sizes at IP should be $\sigma_y$=2.6nm and $\sigma_x$=240nm. The LC needs to produce

low emittance beams, accelerate them without excessive emittance dilution and focus them to the tiny size required.

There are several proposals to preserve the emittance and beam trajectory correction during the beam acceleration, such as the beam based alignment (BBA), the special distribution of energy deviation along a single bunch (BNS) damping, active feedback systems and others. All of them are based on measurements of the real beam position, the bunch length and the beam phase. The alignment of the main linac quadrupoles and RF structures to the beam will be supported by high-precision beam position monitors captured in the bore of each quadrupole and at two locations near each RF structure. The BPM resolution in the main linac should be less than 0.5 micron. The static offset of 2 microns between quadrupole centers and BPM centers produces the 35% dilution of single-bunch emittance [1]. It means that the accuracy of BPM center should be less than 1 micron. For the final focus system where the beam size comes down to 3 nm in the vertical direction, the BPM resolution in this direction should be less than the beam size and should be as small as 1 nm. The systematic phase error of one degree of X-band main linac produces 0.3% final energy error and 0.15% rms final energy spread. This value defines the resolution of phase sensor and it should be better than 1 degree at frequency of 11.424 GHz.

The beam instrumentation for LC has been developed at several laboratories in the world. Most outstanding experimental results were obtained at Stanford Linear Accelerator Center (SLAC) and High Energy Accelerator Researcher Organization (KEK), BINP Protvino. TESLA Hamburg was also a partner in this work.

## 1.2 Resolution and accuracy of different type of sensors

BPMs to be used in a liniar accelerator and damping rings at present time include: button type BPMs [10], high frequency button BPMs, stripline BPMs [11], cavity BPMs [2,3,4,8,13,17] and BPMs using damped slot cavities.

A cylindrical beam-position monitor used in many accelerator facilities has four pickup buttons (BBPM) (See Fig. 1-1) with angle of 90 degrees between neighboring buttons on which the beam image current is induce by bunched beam signals. These probe-electrode signals are

geometrically configured to provide beam-position information in the two orthogonal directions.

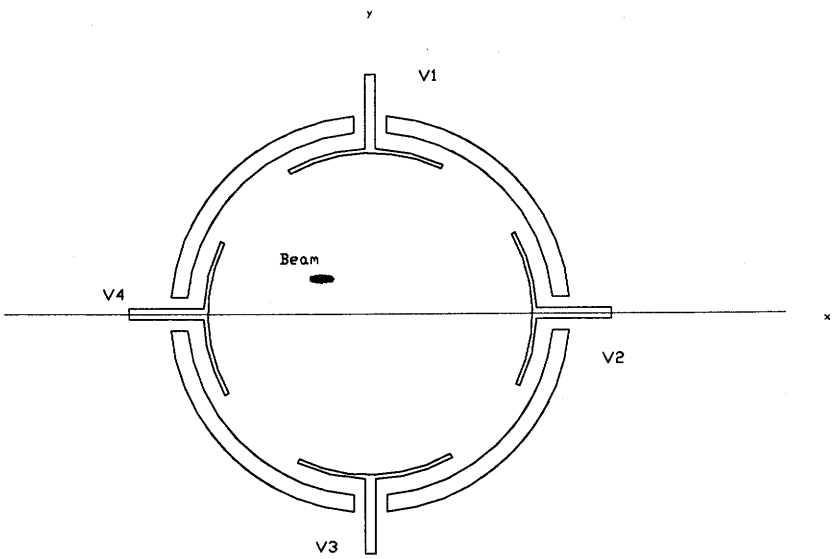


Figure 1-1: Four bottons beam position monitor.

An electronic processor performs a mathematical transfer function (TF) on these BPM electrode signals to produce output signals whose time-varying amplitude is proportion to the vertical and horizontal positions of the beam [9]. A single electrode of a BBPM pickup delivers a signal voltage

$$Vpick = s(x,y) \bullet Z(\omega) \bullet I_{beam}(\omega), \qquad (1.2)$$

which is proportional to the beam intensity, $I_{beam}(\omega)$, and to the beam-to-electrode distance (x, y), expressed by a sensitivity function $S(x,y)$. The transfer impedance Z (ω) depends on the pickup geometry and its on-axis (x=0, y=0) value is used normally.

For the circular cross-sectional BPM detecting horizontal thin beams, sufficient information on beam position can come from four pickups as

$$\begin{aligned} U_x &= k_x(V_2 - V_4)/(V_2 + V_4), \\ U_y &= k_y(V_1 - V_3)/(V_1 + V_3), \end{aligned} \qquad (1.3)$$

where $U_x$ and $U_y$ are calculated values of the beam offset in the horizontal and the vertical directions, respectively, $k_x$ and $k_y$ are the

scaling factors , $V_2$ and $V_4$ are the output voltages from horizontal buttons, $V_1$ and $V_3$ are the output voltages from the vertical buttons.

A resolution of BBPM can be as good as few micrometers and can be even improved by using more wide-band electronics circulars. So-called
high frequency BPMs (HF BPM) in the ATF have resolutions of about 15μm, and it is possible to achieved 2 μm resolution by using 714MHz electronics circuits. The spectrum signal from this BPM is shown in Fig.1-2.

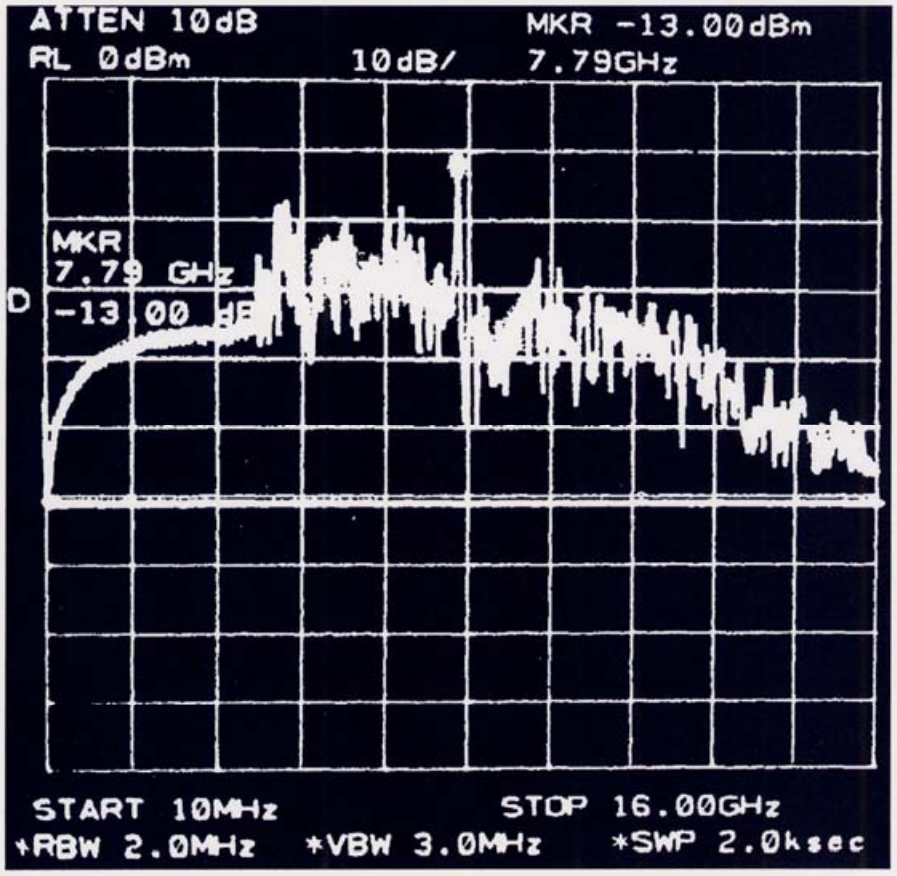


Figure 1-2: Spectrum from botton type BPM of the ATF.

This type of BPM has an offset of the electrical center relativity to the mechanical one of the order of ~ 90 μm standard deviations in both directions [5]. The main source of this offset comes from errors in the manufacture of the BPM block and especially from brazing technology of feedthroughes to the BPM block.

Stripline BPM (SBPM) has the cross sectional view similar to that of Fig. 1-2, but its sensor plates has much longer electrodes in the beam

direction. The resolution of this type of BPM can be as good as a few hundreds of nm [10], because the capacities of pickup to beam are larger. However, the accuracy of the center is similar to that of BBPM because it uses the same technology for feedthrough brazing. One possibility to increase the center accuracy is proposed [11]: the pickup electrodes are formed in the inside of a ceramic tube by cutting out aluminized surface and thus it is free from the limitation due to the brazing technology. However the dielectric constant of ceramic is usually large so that we expect an increase of the longitudinal impedance.

The performance of the RF cavity BPMs was tested by two groups: at the Brookhaven National Laboratory (ATF) by BINP group [3,17] and at SLAC Final Focus Test Beam (FFTB) by T. Shintake group [4, 8]. The Shintake group used three C-band (5.712GHz) cylindrical cavities and one reference cavity closed in one set. The FFTB beam has the energy of 47 GeV, the vertical beam size of 70 nm and the vertical beam position jitter of about 140nm at the place where BPM triplet was located. They reported that the measured position resolution is approximately 25nm; note that this group measured only the vertical beam position.

The BINP group used three K-band (14.000GHz) sensor cavities and one reference cavity. All sensor cavities were installed on movers that can move sensors in both the horizontal and the vertical directions. The BNL ATF had the energy of 80 MeV, the vertical beam size of 10 micrometers and the vertical position jitter of about 25 micrometers in the BPMs setup place. This group reported that the position resolution was measured to be approximately 150 nm.

These two experiments are very good examples that demonstrate the very high resolution of RF cavity BPMs.

# Chapter 2

# Sensors of the bunch position and bunch phase.

## 2.1 Principle of the cavity sensor for measurements of the bunch position

The main idea to use a cavity as a sensor for the bunch position measurement was proposed in 1960's. Such type of sensors were installed at Stanford Linear Accelerate where the rectangular-shape resonators were used for measurement of the bunch position and a cylindrical cavity with TM010 mode was used for measurements of the current [12]. In 1980's, such type of sensor gained more interest as discussion on the prospects of creation of Linear Collider on Tev range energy begun. These types of colliders need very small beam sizes in the interaction point and thus the measurement of the beam position with high resolution and high accuracy is necessary. In the works [2, 3, 4, 7, 8, 10, 12 and 15], different ways to realize cavity sensors were proposed for bunch position measurements in Linear Colliders.

The principle of the cavity sensor for the position of the bunch [2, 4,10,12,15] can be summarized as this: a bunch of charged particles passes through the cavity and leaves a small fluction of its energy, which is proportional to its charge (the symmetrical modes of the cavity), the offset of the bunch relative to the center of the cavity (the asymmetrical modes), the angle between the axis of the cavity and the trajectory of the bunch in the cavity (the magnetic modes in the cavity), and to the tilt of the bunch due to bunch length. Figure 2-1 shows a beam position sensor working at the first nonsymmetrical mode (TM110) were r is the radius of the cavity and h is its length.

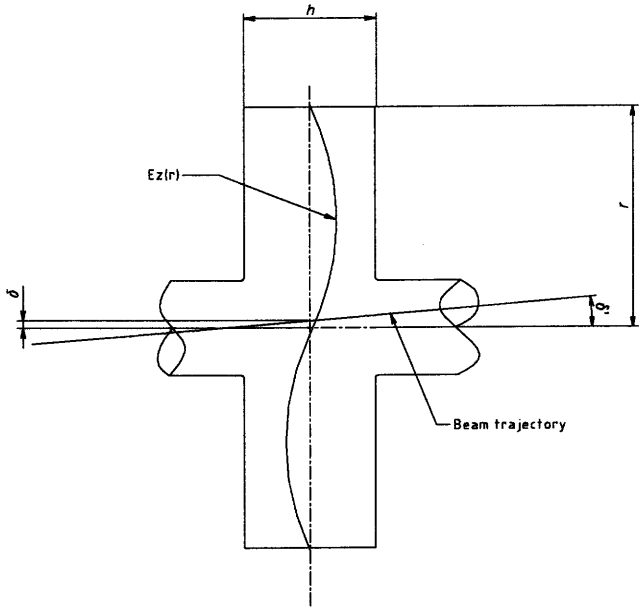


Figure 2-1: Cavity BPM model. TM110 mode.

The voltage generated by a charged bunched beam when it passes through the cavity (electron or positron) can be written as

$$V(d\omega) = q(A_1(\omega)\delta + jA_2(\omega)\delta' + jA_3(\omega) + V_{noise}(d\omega)), \quad (2.1)$$

where $d\omega$ is the frequency band-pass of the receiver, $q$ is the beam charge the functions $A_i(\omega)$ $(i = 1, -3)$ correspond to their determination modes in the cavity and their magnitudes depend on the coupling factor between the electromagnetic fields of the passing beam and the cavity fields of each mode. We assume that the system uses coupling pickup antenna followed by a band –pass filter. The first term of Eq. (2.1) is the beam position signal which is basically in the phase component of TM110 mode. It is proportional to the beam offset $\delta$ and the beam charge. The second one is proportional to the beam trajectory angle $\delta'$ relative to the cavity axis. This signal is 90 degree out-of-phase from the beam current. The third term is the common mode leakage of TM010 mode through the band–pass filter due to the limiting cavity Q factor and it has the 90 degree out-of-phase current in the cavity. The fourth term is the thermal noise in the detector electronics.

Let us consider the general expression of the fields in a cylindrical cavity. The cylindrical cavity is formed by cutting a round waveguide and attaching two end plates with ideal conductivity on its both sides. The field components for magnetic modes in the cavity can be written as [18]:

$$E_r = -iC\frac{\omega\mu\mu_0}{k_{\lim}^2}k_\varphi\frac{J_n(rk_{\lim})}{r}\sin(k_\varphi\varphi)\sin(k_z z),$$

$$E_\varphi = iC\frac{\omega\mu\mu_0}{k_{\lim}^2}k_\varphi J'_n(rk_{\lim})\cos(k_\varphi\varphi)\sin(k_z z),$$

$$Ez = 0,$$

$$H_r = C\frac{k_z}{k_{\lim}}k_\varphi J'_n(rk_{\lim})\cos(k_\varphi\varphi)\cos(k_z z),$$

$$H_\varphi = C\frac{k_z k_\varphi}{k_{\lim}^2}k_\varphi\frac{J'_n(rk_{\lim})}{r}\sin(k_\varphi\varphi)\cos(k_z z), \quad (2.2)$$

$$Hz = CJ_n(rk_{\lim})\cos(k_\varphi\varphi)\sin(k_z z).$$

For electrical modes, the field components can be written as:

$$
\begin{aligned}
E_r &= -C\frac{k_z}{k_{\lim}} J'_m(rk_{\lim})\cos(k_\varphi \varphi)\sin(k_z z), \\
E_\varphi &= -C\frac{k_z k_\varphi}{k^2_{\lim}} \frac{J_m(rk_{\lim})}{r}\sin(k_\varphi \varphi)\sin(k_z z), \\
E_z &= CJ_n(rk_{\lim})\cos(k_\varphi \varphi)\cos(k_z z), \\
H_r &= iC\frac{\omega\varepsilon\varepsilon_0 k_z}{k^2_{\lim}} \frac{J_m(rk_{\lim})}{r}\sin(k_\varphi \varphi)\cos(k_z z), \qquad (2.3) \\
H_\varphi &= -iC\frac{\omega\varepsilon\varepsilon_0}{k_{\lim}} J'_m(rk_{\lim})\cos(k_\varphi \varphi)\cos(k_z z), \\
H_z &= 0,
\end{aligned}
$$

where $C$ is the field magnitude, $k_\varphi = n/\pi$ , $k_z = m\pi/h$ and $k_{\lim} = \nu_{mn}/a$ , are the wave numbers, $a$ and $h$ is the radius and length of the round waveguide, $\nu_{nm}$ and $\nu'_{nm}$ are the $n_{th}$ -root of Bessel function $J_m(x)$ and its derivative $J'_m(x)$ of order $m$, respectively, $\omega$ is the angular frequency, $\mu\mu_0$ and $\varepsilon\varepsilon_0$ are the magnetic and electric constants, respectively. Figures. 2-2, 2-3 and 2-4 show magnetic field lines in the cylindrical cavity for the first three modes, respectively.

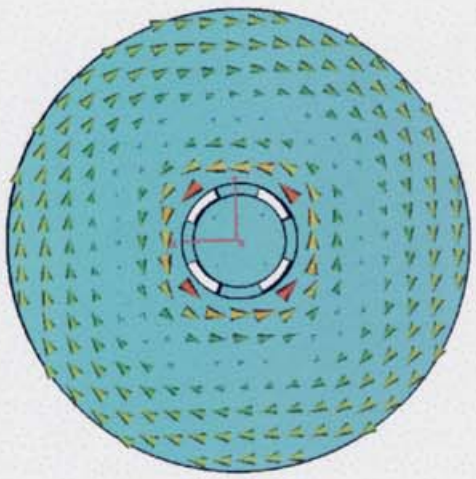

Figure 2-2: Magnetic field lines of TM020 mode.

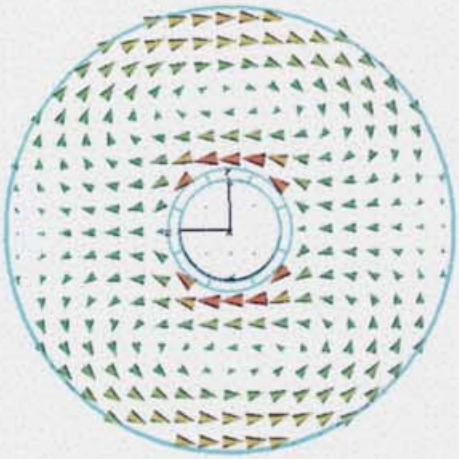

Figure 2-3: Magnetic field lines of TM110 mode.

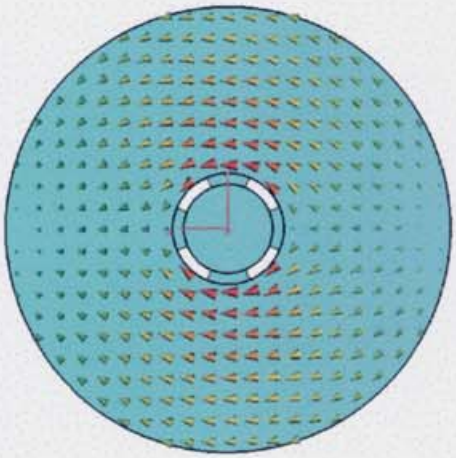

Figure 2-4: Magnetic field lines at mode TE110

From Eqs. (2.2) and (2.3) and using the boundary conditions, one can find that the resonance frequencies for the TE modes can be written as:

$$\omega_{mnp} = \frac{1}{\sqrt{\mu\mu_0\varepsilon\varepsilon_0}}\sqrt{\left(\frac{\nu'_{mn}}{r}\right)^2 + \left(\frac{p\pi}{h}\right)^2} \quad . \quad (2.4)$$

For the TM modes, we have

$$\omega_{mnp} = \frac{1}{\sqrt{\mu\mu_0\varepsilon\varepsilon_0}}\sqrt{\left(\frac{\nu_{mn}}{r}\right)^2 + \left(\frac{p\pi}{h}\right)^2} \quad . \quad (2.5)$$

The beam position can be measured using the TM110 mode. The electrical and magnetic fields of the TM110 mode are

$$E_z = CJ_1(k_{11}r)\cos(\varphi),$$
$$H_z = -j\frac{CJ_1(k_{11}r)}{\omega\mu r}\sin(\varphi),$$
$$H_\varphi = -j\frac{Ck_{11}J'(k_{11}r)}{\omega\mu}\cos(\varphi), \qquad (2.6)$$

where, $k_{11} = \nu_{11}/r$ is the wave number of the TM110 resonance, $\nu_{11}$ is the first root of the Bessel function $J_1(x)$, and

$$C = \frac{V1}{hJ_{1\max}},$$

where $V1$ is the voltage in the cavity at the radius at which the Bessel function has the maximum $J_{1\max}(x)$. All other field components of this mode are zero.

For description of the interaction of the bunch with the cavity, we shall present the cavity as the equivalent circuit. In Fig. 2-5, $L$ is the inductance of the cavity, $R$ is a resistance of the cavity defining its Q factor, and $C$ is the capacitance of the cavity through which the interaction between the bunch fields and the cavity take place.

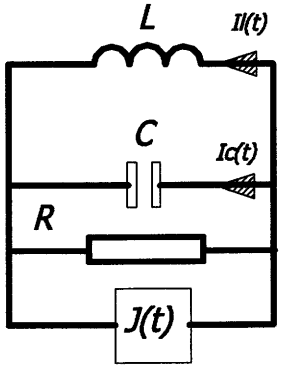


Figure 2-5: Equivalent circuit of monitoring cavity.

The $Q$ factor of the cavity is given by

$$Q = 2\pi \frac{Wc}{W_{loss}} = \omega_0 \frac{Wc}{P_{loss}} , \quad (2.7)$$

where $W_c$ is the energy stored in the magnetic and electrical fields of the cavity. Here

$$W_{loss} = P_{loss} T_0 \quad (2.8)$$

is the energy diffused in the cavity for one period $T_0 = 2\pi / \omega_0$ and $P_{loss}$ is the energy diffused in the active resistance of the cavity, and $\omega_0 = 2\pi / T_0$ is the angular frequency. Suppose that the cavity has the volume $V$ and surface area $S$. From the Gaussian theorem, we have

$$\oint_S \varepsilon\varepsilon_0 E dS = q , \quad (2.9)$$

where $q$ is the total charge inside of the volume $V$. The stored energy in the cavity of the volume $V$ can be calculated as

$$Wst = \int_V \frac{\varepsilon\varepsilon_0 |E_{\max}|^2}{2} dV , \quad (2.10)$$

or

$$Wst = \int_V \frac{\mu\mu_0 |H_{\max}|^2}{2} dV . \quad (2.11)$$

In the equivalent circuit, the stored energy in the cavity is given by

$$W_e = \frac{CU^2}{2} , \quad (2.12)$$

where $U$ is the voltage difference between both sides of the capacitance and it is equal to $q/C$. Other parameters of the equivalent circuit are given by

$$C = \varepsilon\varepsilon_0 \frac{\oint_S EdS}{\int_V |E_{\max}|^2 dV}, \quad (2.13)$$

$$L = \frac{\int_V |E_{\max}|^2 dV}{\omega_0^2 \varepsilon\varepsilon_0 \oint_S EdS}. \quad (2.14)$$

If we know the particle trajectory in the cavity and if we know the fields inside this cavity, we can then calculate the equivalent cavity voltage by simple line integral of the electric field in the cavity axis

$$U_p = -\int_l E_{\max} dl, \quad (2.15)$$

where $l$ is the particle trajectory and $Emax$ is the electric field on the cavity axis. From this voltage and the cavity losses, we can write down formulae for cavity shunt impedance

$$R_{sh} = \frac{\left[\int_l E_{\max} dl\right]^2}{2P_{loss}}, \quad (2.16)$$

$$\text{or} \quad R_{sh} = \frac{\left[\int_l E_{\max} dl\right]^2}{2\omega_0 W_{st}} \quad Q = \frac{\left[\int_l E_{\max} dl\right]^2 Q}{\omega_0 \int_V \mu\mu_0 |H_{\max}|^2 dV}. \quad (2.17)$$

Usually more convince expression for the shunt impedance in terms of its square is used

$$\left(\frac{Rsh}{Q}\right)^{1/2} = \frac{[\int_l E_{\max} dl]}{\sqrt{\omega_0} \int_V \mu\mu_0 |H_{\max}| dV}. \quad (2.18)$$

Let us see the interaction between the beam and the cavity and introduce this interaction as a part of energy transmission through the cavity longitudinal impedance. From Shokly-Romo theorem [20], if the charge has velocity $v$ and is moving in the field of system of electrodes which have the potential $U$, the circuits (see Fig. 2-5) of this electrode excite the current $J(t)$ given by

$$J(t) = qv\frac{-\overline{E}(x(t))}{U}, \qquad (2.19)$$

where $E$ is the electric fields of the potential $U$.
Let us calculate the voltage [10] excited by the beam when it passes in parallel to the cavity axis and the beam has a displacement of $\delta$ to the axis. From the energy-conservation law, work done by the beam is equivalent to the increase of the stored energy in the capacitance $C$ in Fig. 2-5. Considering Eqs. (2.13) and. (2.15), we can write

$$dV(\delta) = \frac{1}{CU_p}\int_{-\infty}^{+\infty} qEvdt, \qquad (2.20)$$

or using Eq. (2.18),

$$dV(\delta) = q\omega(R/Q)^{0.5}T(\varphi_b)\frac{J_1(k_{11}\delta)}{J_{1\max}}M_{cav}, \qquad (2.21)$$

where $q$ is the beam charge, $\omega^2 = \frac{1}{LC}$ is angular frequency of the cavity, $C$ is the equivalent capacitance of the cavity, $T(\varphi_b)$ is the beam coupling coefficient, $\varphi_b = \sigma_b\omega/c = (\sigma_b/T)/(2\pi/c)$ is the beam phase, $M_{cav} = \sin(\varphi_{cav}/2)/(\varphi_{cav}/2)$ is the transient time factor for the cavity, $\varphi_{cav} = h\omega/c = (h/T)/(2\pi/c)$ is the cavity phase, $k_{11}$ is the wave number for TM110 mode and $h$ is the effective cavity length.

For the output voltage from the sensor cavity with real coupling coefficient $\beta$, we can write

$$V_{11}^{out}(\delta) = V_{11}(\delta)\beta\left(\frac{R_{load}}{Q_l}\right)^{0.5}, \quad (2.22)$$

where $\beta$ is the coupling coefficient between the outputs port and the cavity, $R_{load}$ =50 Ohm, $Q_l$ is the loaded $Q$ factor. The beam coupling coefficient for the linear distribution of the charge over the bunch length can be written as

$$T(\varphi_b) = \frac{\sin(\varphi_b/2)}{\varphi_b/2}. \quad (2.23)$$

The beam coupling coefficient in case of the Gaussian distribution of the charge over the bunch length can be written as [16]

$$T(\varphi_b) = \exp(-\varphi_b^2/2). \quad (2.24)$$

From the Eq. (2.21) with Eqs. (2.22) and (2.24), we can see that the output voltage from the cavity is linearly proportional to the beam charge, the displacement of the beam trajectory from the cavity axis, and depends also on the beam length.

The resulting formula for the cavity output voltage can be written as:

$$V(\delta) = q\omega(R/Q)^{0.5}\frac{\sin(\varphi_{cav}/2)}{\varphi_{cav}/2}\frac{J_1(k_{11}\delta)}{J_{1\max}}\exp(-\varphi^2{}_b/2)\beta\left(\frac{R_{load}}{Q_l}\right)^{0.5}. \quad (2.25)$$

## 2.2 Main design and estimation of accuracy and tolerance

For study of nature of beam jitter due to unstable extraction kicker at the KEK ATF, the RF cavity beam position monitors were suggested to install in the ATF extraction line. These monitors should have the resolution of less then 0.5 microns (the existing BPMs in the ATF extraction line do not have enough resolution to measure this beam jitter). The knowledge of the proper values of bunch coordinate could be used for more exact beam emittance calculation. The emittance measurements in the ATF extraction line are carried out by means of wire meter. The diameter of the wire is of the order of 10 microns. The beam position resolution of the existing position sensors is about 15 microns which is more than the diameter of the wire. Therefore these monitors could not be used for measurements of bunch coordinate. To study the accuracy and resolution of position measurement by the RF cavity bunch sensors themselves, it was suggested to install three cavity sensors and one reference cavity to the ATF extraction line. The parameters of an electron bunch in the ATF extraction line are summarized in Table 2-1.

The operation frequency of the cavity sensor was chosen to be the $18^{th}$ harmonic of the bunch spacing frequency. It is 6,426MHz. The frequency choice was mode based on the low price of RF electronics for measurements at this frequency. Figure 2-6 shows the general view of the cavity sensor.

Regarding the BPM system chipsets, each BPM has two outputs, one for horizontal and another for vertical signals coupled with detection electronics by RF cables. For fine tuning of the frequency of the cavity, the thermal heating can be used. Each cavity sensor has an individual heater and temperature sensor with feedback for temperature stabilization, which automatically keeps the frequency to the desired value.

As shown in Eq. (2.25) in Chapter 2-1 for the cavity with TM110 mode, the output signal amplitude is proportional to the beam displacement from the cavity axis and to the value of charge. But it also depends on the bunch length that, like all real beam parameters, has jitter as well. The working frequency of the reference cavity was chosen to be equal to the

sensor cavity frequency (6,426 MHz) and it also corresponds to the 18$^{th}$ harmonic of bunch spacing frequency. Figure 2-7 show the general view of the reference cavity. To make the Q factor as big as possible and to have the possibility to measure the bunch length, the reference cavity was made oversized. The frequency of 6,426 MHz corresponds to the second symmetrical mode, TM020. The frequency of TM010 is 2,856 MHz and this is the 8$^{th}$ harmonic of the bunch spacing frequency. The data for beam coupling coefficient versus the bunch length is plotted in Fig. 2-8. It is clear from this figure that the magnitude of mode TM010 practically does not depend on the bunch length and it is possible to use its value for normalization of bunch length. Since the frequency of this mode is the harmonic of the bunch spacing, the normalization can be also used in multi-bunch mode. To make the frequency of TM020 mode to be equal to the twice the frequency of TM010 mode, we use the addition hole located in one side of the cavity. The electric field patterns of the TM010 mode and TM020 mode are shown in Figs. 2-9 ($a$) and ($b$), respectively. The parameters of the reference cavity for calculation with the code SLANS is tabulated in Table 2-2.

The beam coupling factor for the linear and Gaussian charge distributions along the bunch is shows in. Fig. 2-10. The basic parameters of cavity sensor are shown in Table 2-3. The electric field pattern of TM110 is plotted in Fig. 2-11. Figure 2-12 shows the model for calculation of the cavity sensor parameters. The estimation of sensitivity was done using Eq. (2.27) in Chapter 2.1. The frequencies and the Q factors of the first six modes are given in Table 2-4. The reflection coefficient for one of cavity coupling port is shown in Fig. 2-13 at the resonance frequency of 6,426 MHz. The parasitic transmission between X and Y ports in the cavity sensor is shown in Fig. 2-14.

The cavity sensor has the cylindrical shape and it can be fabricated with machinig accuracy of several microns. The machining tolerance of coupling slots can be as big as 20 micron. However, because our cavity has low coupling factor, it does not influence too much on the displacement of the electrical and mechanical centers of the cavity. To make the cavity more axis-symmetrical, we use one additional blank slot which has the same volume as coupling slots to take into account the field leakage. The main error in the displacement of mechanical and electrical center comes from the technology tolerance of brazing between the cavity body and the covered plate. The measured value of the position error of the cavity body and the covered plate is about 15 microns. Taking into account all these factors, the displacement of the electrical and the mechanical centers of the cavity can be as large as 20 micron. However, we do not have an exact measured value up to data.

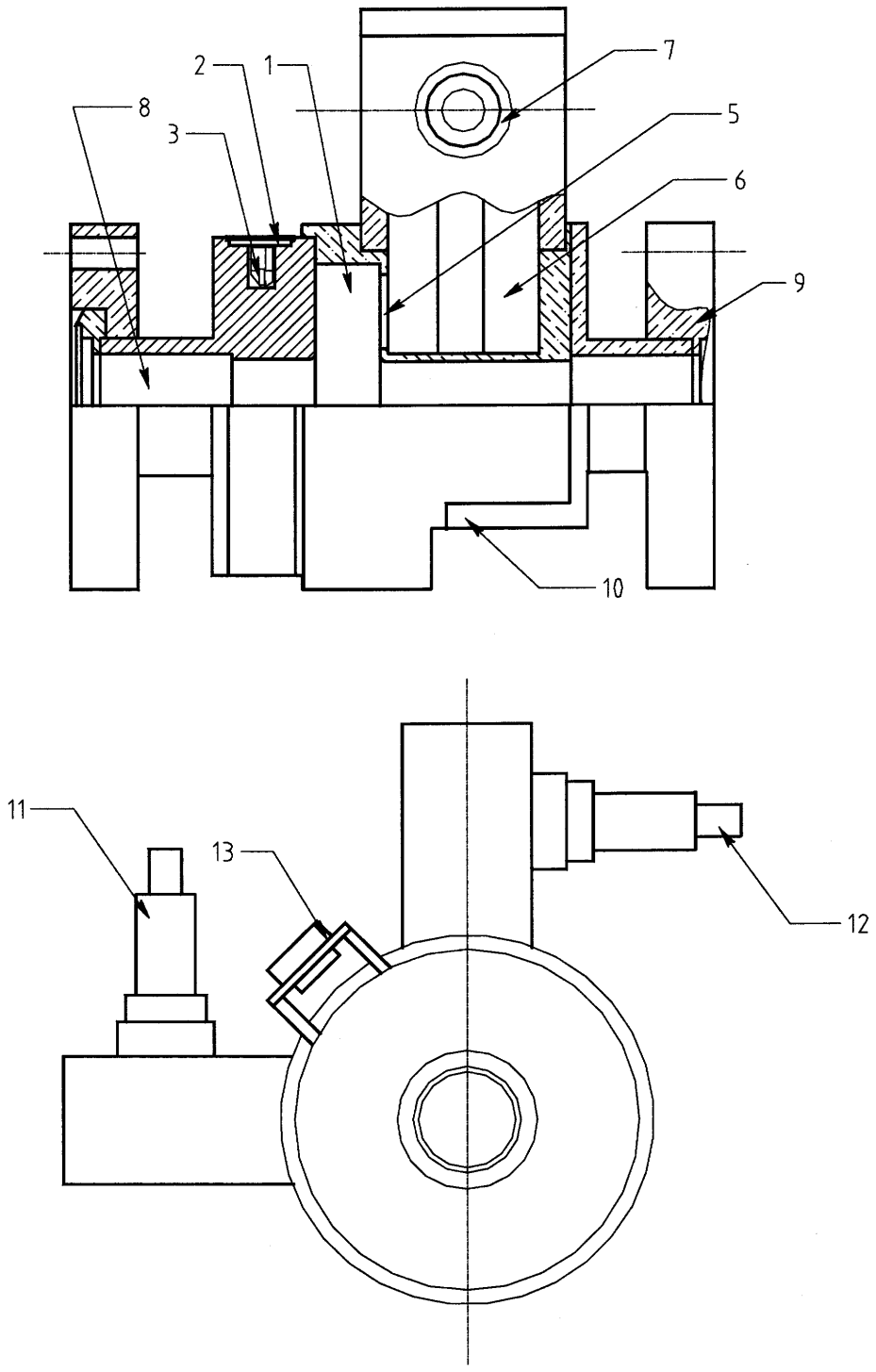


Figure 2-6: Cross-sectional view of cavity BPM.

1.- Cavity sensor . 2- Heater. 3 – Temperature sensor. 5 – Coupling slot. 6 – Output waveguide. 7 – Output feedthrough. 8 – Beam pipe. 9 – Vacuum flange. 10 – Support plate. 11 – Y position output. 12 - X position output. 13 – Heater control connector.

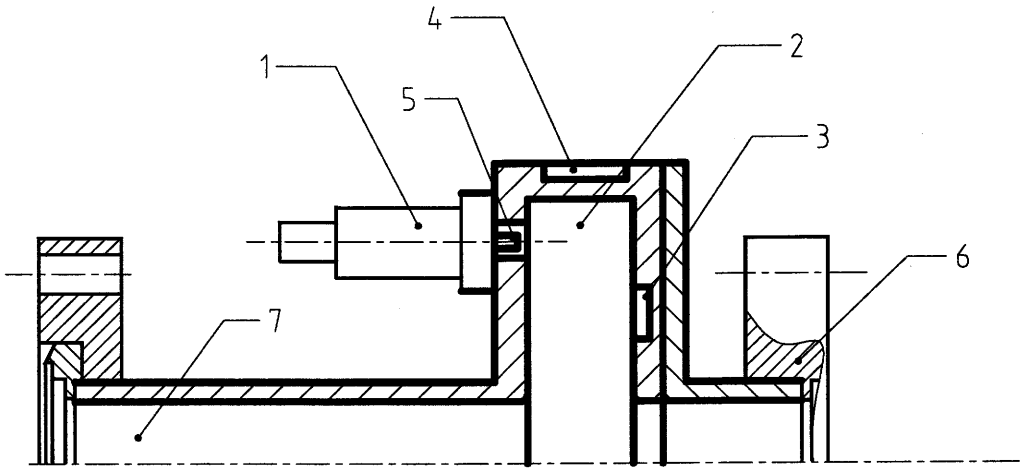


Figure 2-7: Reference cavity.
1 – Feedthrough. 2 – Sensor cavity. 3 – Hole for tuning frequency to TM010 and TM020. 4 – Heater. 5 – Coupling bore. 6 – Vacuum flange. 7 – Beam pipe.

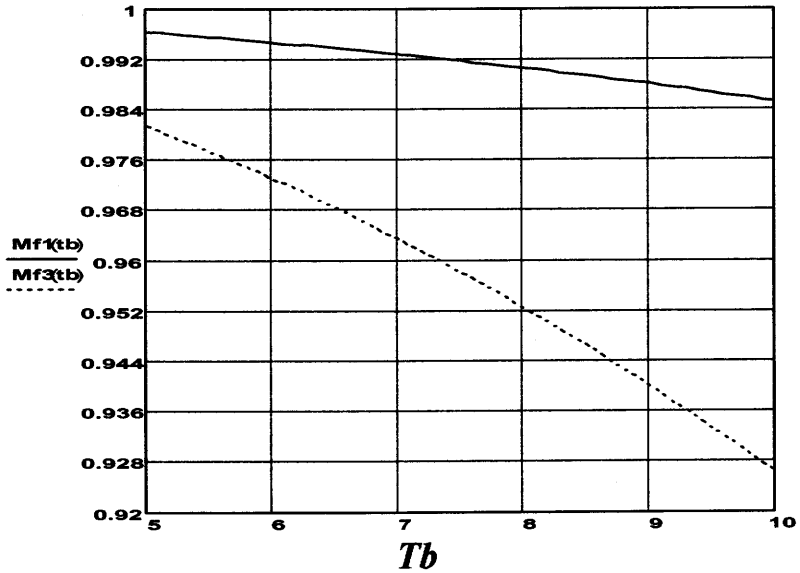


Figure 2-8: The value of bunch coupling factor versus the bunch length for reference cavity. The linear distribution of the charge over the bunch length is assumed. *Tb* - is the bunch length (mm), *Mf1 (Tb)* is for the mode TM010 at frequency of 2,856MHz, *Mf2 (Tb)* is for the mode TM020 at frequency of 6,426 MHz.

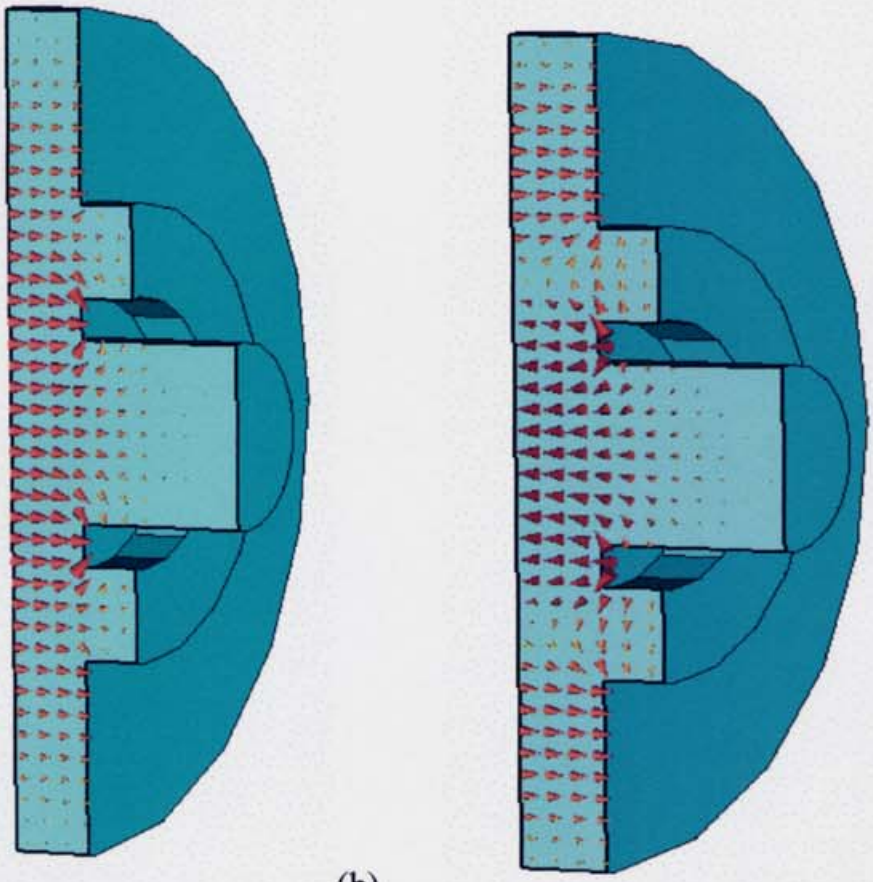

(a) (b)

Figure 2-9: The electrical fields patterns of the TM010 and TM020 modes in the reference cavity.

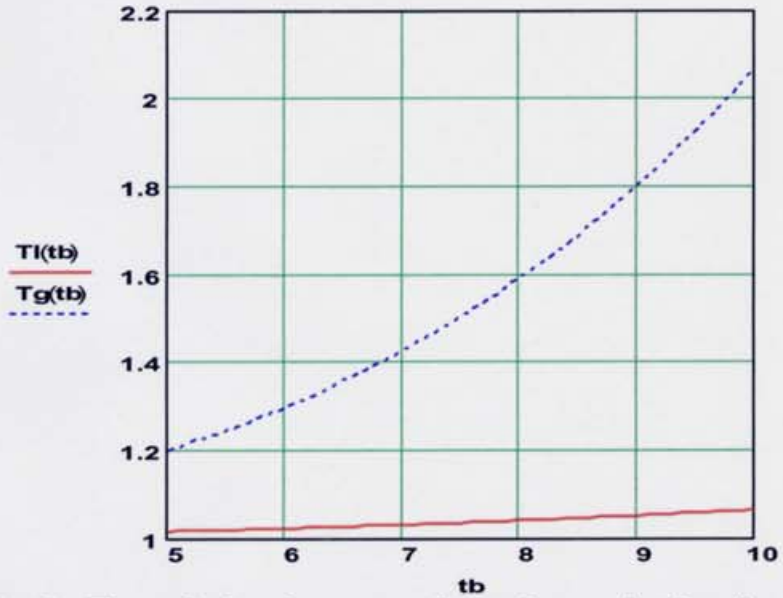


Figure 2-10: The relation between the voltages in the first mode and the voltage in the second mode for differences models of charge distribution along the bunch. Tb is the bunch length (mm), *Tl (tb)* is linear distribution of charge density, *Tg (tb)* is the Gaussian distribution of charge density.

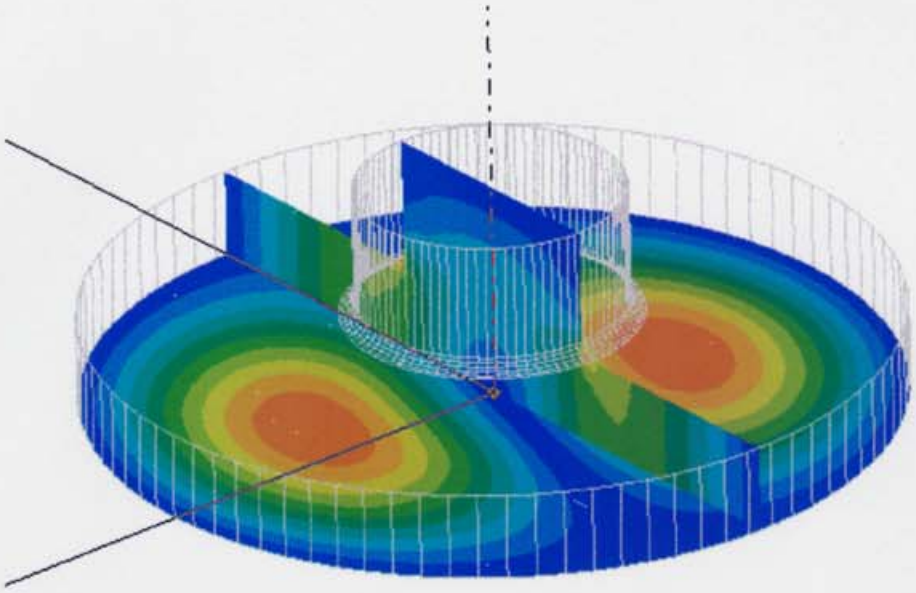

Figure 2-11: Electric fields for one polarization of the TM110 mode in the cavity sensor. The Frequency is 6,426 MHz

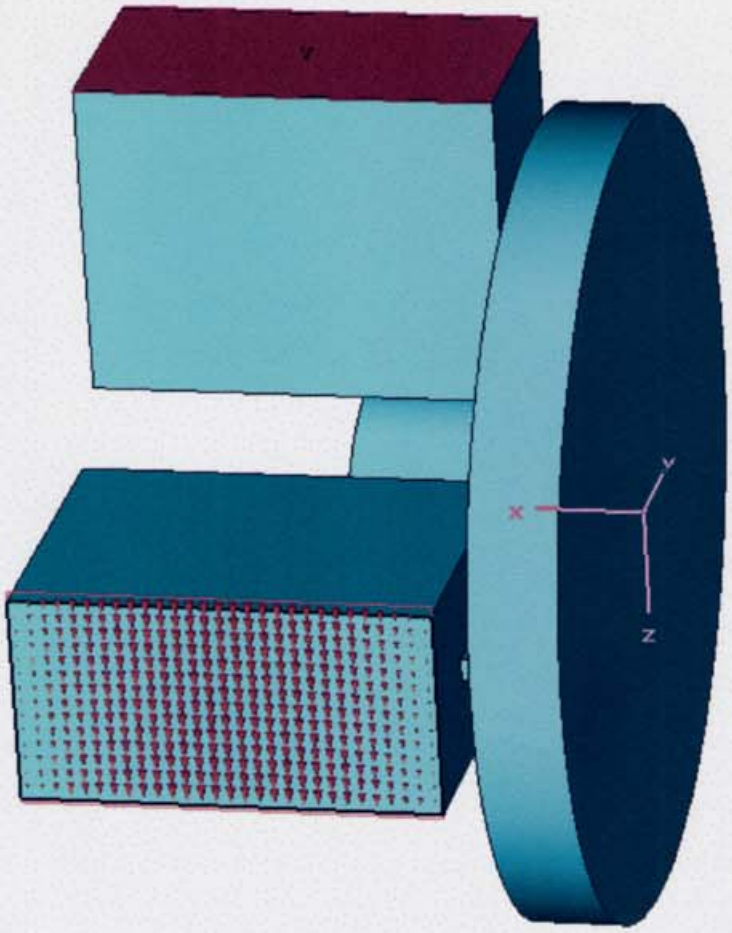


Figure 2-12: Model for calculations of the fields in the cavity sensor.

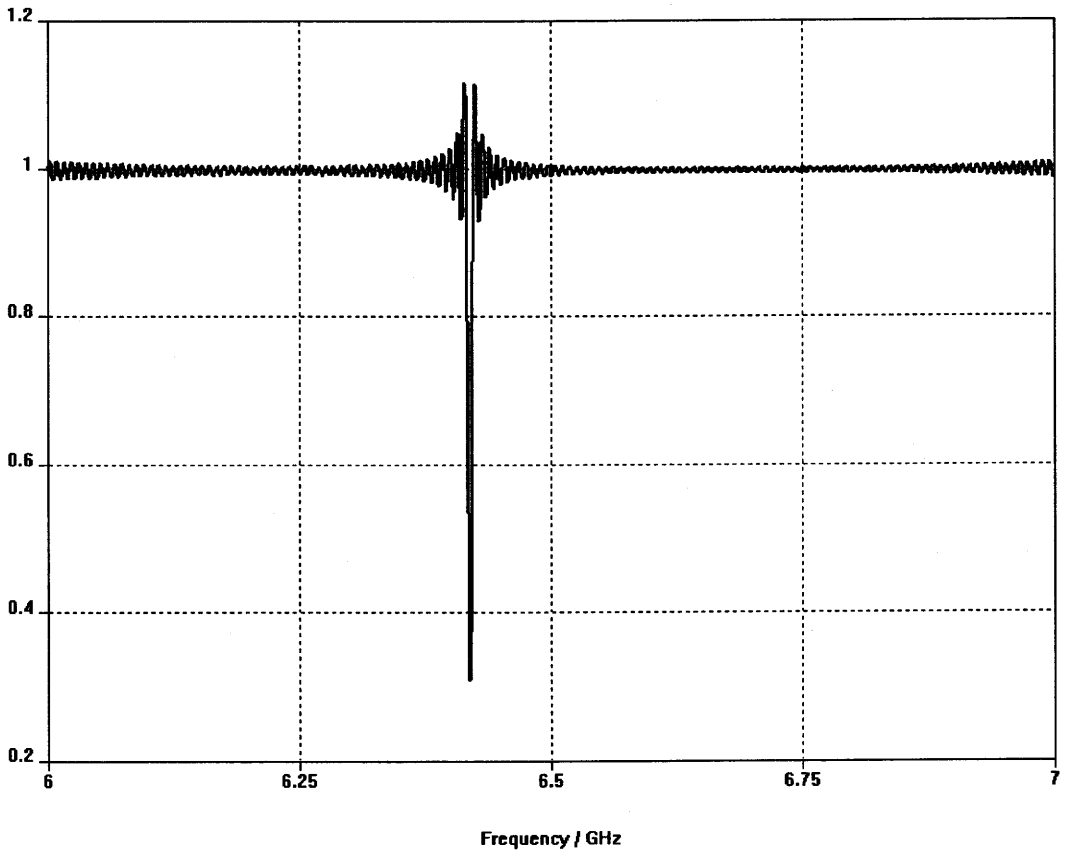


Figure 2-13: Reflection coefficients for port 1 in the sensor cavity.

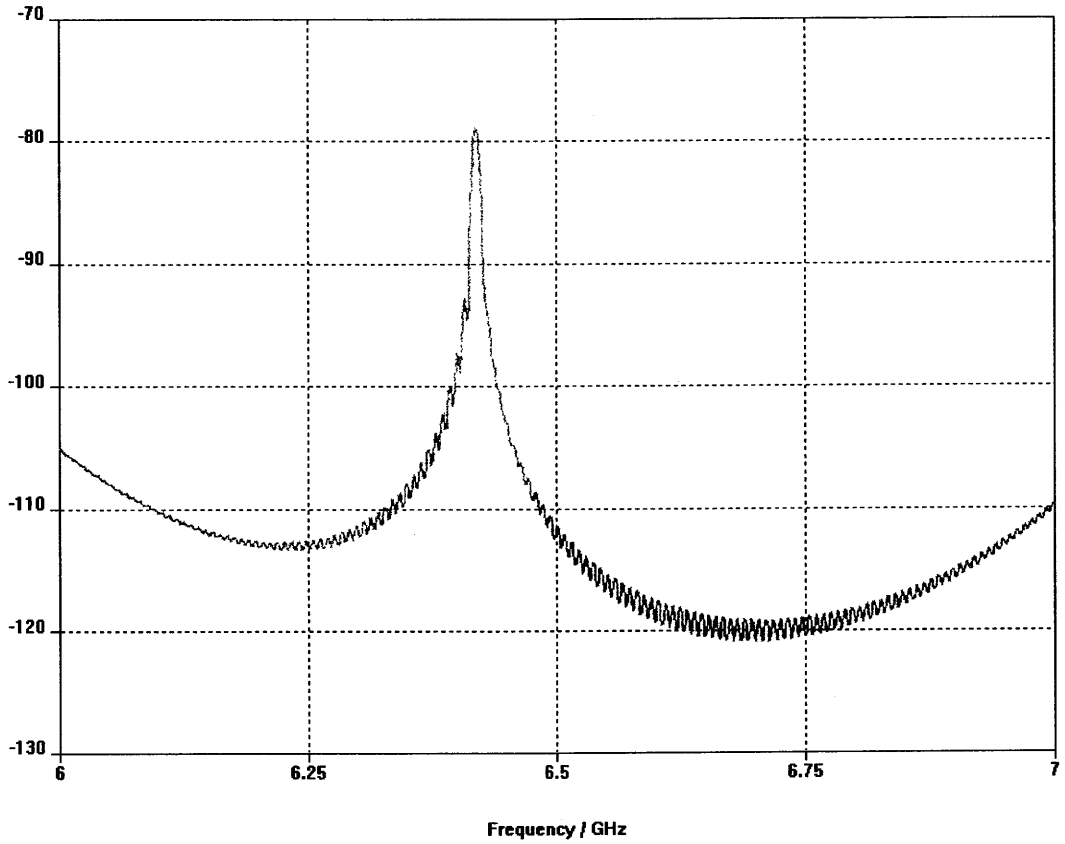


Figure 2-14: Parasitic transmission between X and Y ports in the sensor cavity.

Table 2-1: Parameters of an electron bunch in the ATF KEK.

| | |
|---|---|
| Beam energy | 1.28 GeV |
| Single-bunch population | 1.2E 10 |
| 20 multi-bunch population | 7.6E 10 |
| Bunch length | 7 - 9 mm |
| Horizontal emittance | 2.5Ee-6 |
| Vertical emittance | 2.5E-8 |
| Bunch separation | 2.6E-9 sec |
| Repetition rate | 0.7 – 4 Hz |

Table2-2: Parameters of the reference cavity.

| Mode | TM010 | TM020 |
|---|---|---|
| Cavity radius | 4.15 cm, | |
| Cavity length | 1.6 cm | |
| Slot radius | 1.5 cm | |
| Slot length | 0.6 cm | |
| Slot deep | 0.15 cm | |
| Frequency. | 2.85669E+03 MHz | 6.4265E+03 MHz |
| Length of wave | 10.53128 cm | 4.6681 cm |
| Wave value | 0.5966214 1/cm | 1.3410 1/cm |
| Quality factor | 8.8345E+03 | 9.3261E+03 |
| Transit time factor | .8895 | .51005 |
| Effective impedance | 0.0579E+00 Ohm | 0.2178 Ohm |

Table 2-3: Basic parameters of cavity sensor.

| | |
|---|---|
| Frequency of TM110 mode | 6,426 MHz |
| Wave length | 46.68 mm |
| Cavity radius | 27.11 mm |
| Beam pipe radius | 9 mm |
| Cavity length | 12 mm |
| Slot length | 14 mm |
| Slot width | 1.5 mm |
| Number of slots in cavity | 2 |
| (R/Q) | 27 Ohm |
| Transit time factor | 0.894 |
| Unloaded Q factor | 5,100 |
| Loaded Q factor | 3,300 |
| Output signal into the load 50 Ohm | 20 V/nC/mm |

Table 2-4: The frequencies and unloaded Q factor for first six modes.

| Mode | Frequency (MHz) | Unloaded Q factor |
|---|---|---|
| TM010 | 4,442.4 | 5.22E3 |
| TM020 | 10,210.9 | 8.36E3 |
| TM110 | 6,426 | 6.19E3 |
| TM210 | 8,912.4 | 7.83E3 |
| TE110 | 8,750 | 6.43E3 |
| TE210 | 12,834 | 9.21E3 |

## 2-3 X-band beam phase sensor

The X-band main linac has two tasks: first, to accelerate trains of the bunches to TeV level of energy, and second, to transport the beam through the linac without unacceptable emittance dilution (particularly the extremely small vertical emittance). It is this constraint that results in the most difficult tolerances in the main linac: alignment of RF structures and RF girders, quadrupole alignment, RF structure straightness. In addition to the alignment tolerances, there are tolerances for systematic and random errors of the klystron phase and amplitude. These tolerances are determined by the stability requirements at the end of linac, set by the demands from the detector and the acceptable final energy spread. For the JLC project, the energy spread should be less than 1 percent, which is set by the narrow bandwidth of the final focus system. Furthermore, if misalignments would be coupled with errors in RF phase or amplitude, they can potentially produce an emittance dilution larger than that due to misalignments of the optics only. Such combination of errors could further tighten the linac tolerances.

In the JLC main linac, eight klystrons which power twelve structures are required to have the same phase. A random phase jitter of 10 degrees RMS can results in 1.5% average energy loss and 0.35% RMS beam energy jitter. A systematic phase error in the main linac RF system or injection time error by 1 degree of X-band frequency results in a 0.3% final energy error and a 0.15% RMS final energy spread. Therefore in order to suppress the emittance growth in the main linac due to the phase errors, it is necessary to have a feedback system to control the difference of the phases between the accelerating voltage in structure and the bunch. Figure 2-15 shows such system using signals of residual phases between the bunch and accelerating voltage, and it feedbacks to the phase adjuster installed on the klystrons power input.

Reducing systematic part of phase correction error is potentially important. One of the important system elements to phase correction is the beam phase sensor. A phase sensor must be installed to a group of RF accelerating structures which are powered by the same set of klystrons. The bunch phase sensor must have low impedance and the induction voltage must not depend on the beam position in the sensor. The phase sensor is an important element to feed RF structures in the right phase, but it can be used also as a sensor for the bunch current and the bunch length. These functions are absolutely necessary in particular at the beginning of the operation and for the tuning of the accelerator.

General requirements for the phase stability system of the main linac demand that the phase sensor with the phase detection system must provide information on the phase difference between the bunch and the RF accelerating voltages with accuracy better than 0.5 degree.

Figure 2-16 presents the scheme of the experiment to measure the accuracy of the phase checking system. The experiment uses the part of Delay Line Distribution System (DLDS). The DLDS has pipes of length of order of 55 meters. The first phase sensor and phase detector were installed at the upstream part of ATF linac where the DLDS pipe starts, and they measure the difference between the bunch phase and the phase of the RF voltage at the entrance of the DLDS. Considering that the RF phase in the DLDS is changed only less than 0.5 degrees in one hour due to the temperature change in the ATF linac tunnel, the signal from the DLDS pipe end can be used as the reference signal for the second phase detector that was installed near the other end of the DLDS pipe (downstream side of the linac). This second phase detector measures the difference of the phases between the signal passing through the DLDS and signal at the second phase sensor. Bunch parameters such as the charge and the bunch length are different at the beginning and at the end of the ATF linac on top of the beam jitter in position.

The bunch parameters in the ATF linac can be measured with good accuracy. Comparing the data from the phase detector and on the bunch parameters, it is possible to draw a conclusion about the influence of the bunch parameters on the accuracy of the phase measurement. Figure 2-17 shows the general geometry of the phase sensor.

The insertion of lossy material (absorber in Fig. 2-17) is necessary, since the beam pipe diameter at the ATF is 30 mm and noise at the fourth harmonic of accelerating frequencies (2,856MHz*4=11,424 MHz) generated by klystrons can easily pass through the phase sensor which is operated at the same frequency. Figure 2-18 shows the oscilloscope display of the induced voltage of the magnitude detector when no absorber was installed (old design). The observed stray signal at the fourth harmonic is very erratic: its amplitude depends on how long klystrons are operated at non–stop, and is slowly decreasing from the beginning of week toward the end. But sometimes it suddenly jumps up several times in a week. Figure 2-19 shows the spectrum from the phase sensor without absorber (old design). The noise signal from klystrons at the fourth harmonica can be seen as upper line since the frequency of the pulse repetition rate of klystrons is 25 Hz, while the beam reputation rate is only 0.5Hz. To improve the output signals from the phase sensor, we decided to make a new design of sensor. The frequency spectrum was improved as show in Fig. 2-20 after absorbers were installed (new design). The new phase sensor has much smaller signal at the
fourth harmonic.

The electrical fields pattern for the TM010 mode and TM020 mode are shown in Figs. 2-21 and. 2-22, respectively. The phase sensor uses a cylindrical symmetrical ring cavity with four slots connected with beam pipe, as show in Fig. 2-23. The phase sensor installation in the ATF KEK linac is showed in Fig. 2-24.

The parameters of the phase sensor are summarized in Table 2-5. The cavity with such shape has very low impedance. It has small coupling factor to the beam that is necessary to minimize the disturbance to the beam parameters by week fields in the cavity. The cavity impedance versus the beam pipe slots is show in Fig. 2-25. The output signal from the cavity is obtained through the coaxial feedthrough located in the peripheral of the cavity.

The output coupling factor of this cavity was chosen to be small so that the loaded Q factor remains to be large. And for this purpose, the cavity was made oversized. The first symmetrical mode TM010 has the frequency at 5,712 MHz. It allows this sensor to be used in multi-bunch operational mode. The signal at this low frequency can be used also as reference for measurements of the bunch length. For tuning of the frequency of the sensor, the sensor is equipped with the heater element and the temperature sensor. The installed temperature stabilization system provides the frequency control with accuracy of +/.-0.05 MHz.

## 2-4 Summary

The new type of RF cavity BPMs with very low coupling factor to all symmetrical modes was proposed and designed. The theoretical studies for development of nanometer-resolution RF BPMs are done. The designed cavity allows us to measure the beam position in single-bunch mode as well as in multi-bunch mode. The measurements of the cold models confirmed the calculation.

The phase feedback system for LC was proposed. For this system, the new type of X-band oversized two-mode phase sensor was proposal and designed. This X-band phase sensor can be also used for bunch length measurements as well as for the beam charge measurement. The performance of X-band phase sensor was measured at KEK ATF linac.

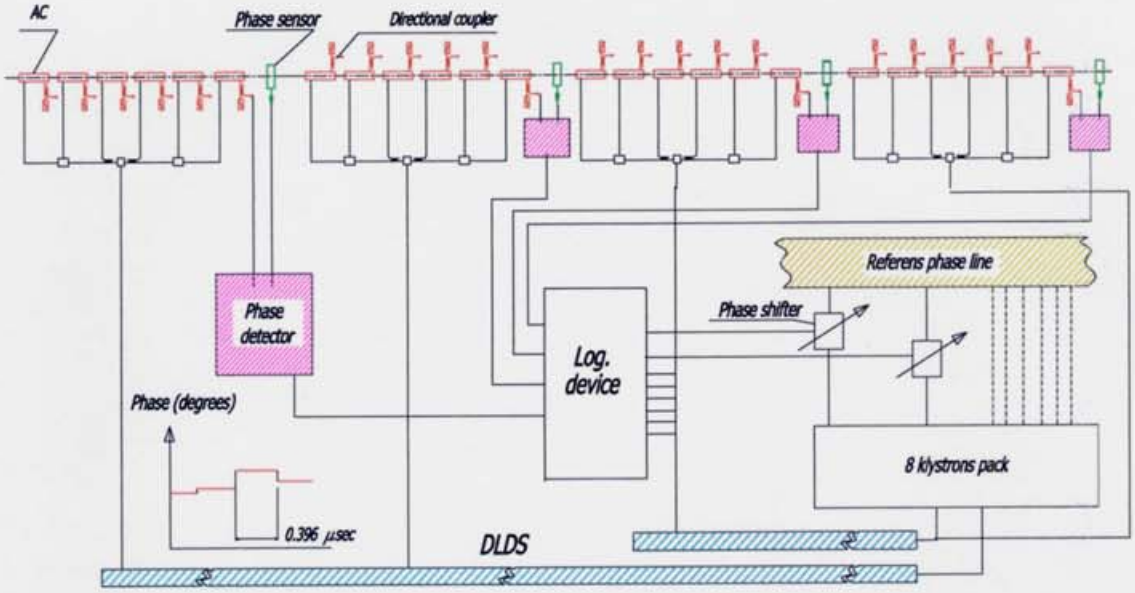


Figure 2-15: Phase stabilization system for LC.

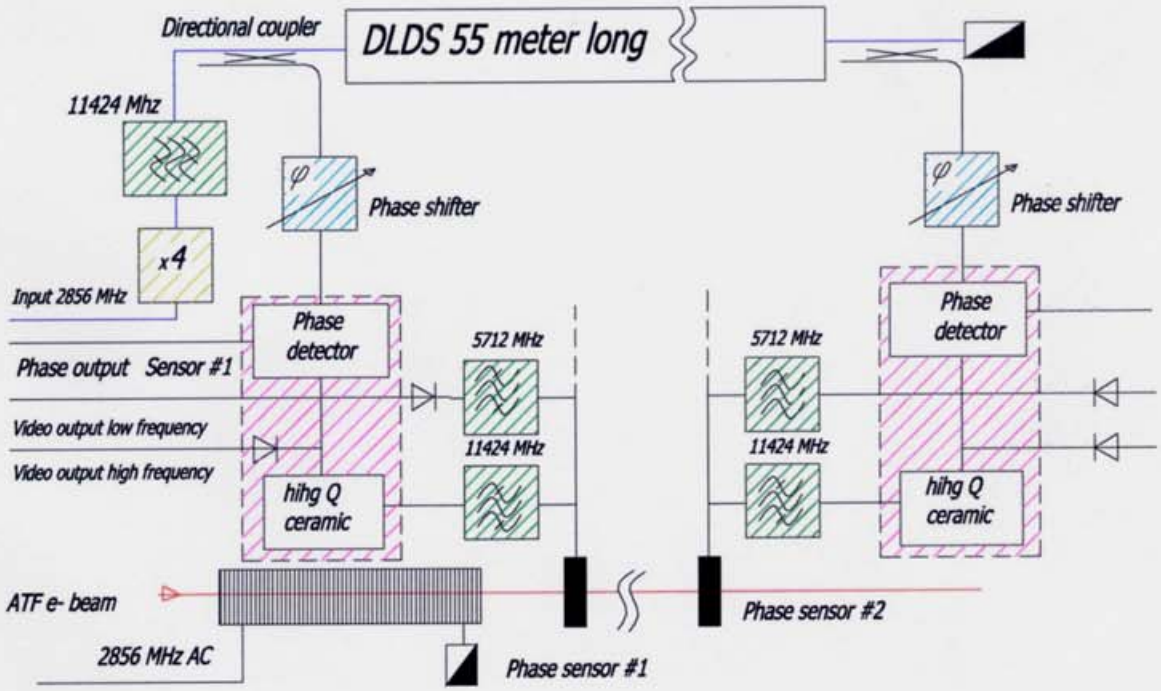


Figure 2-16: ATF beam based experiment for testing of the phase sensor.

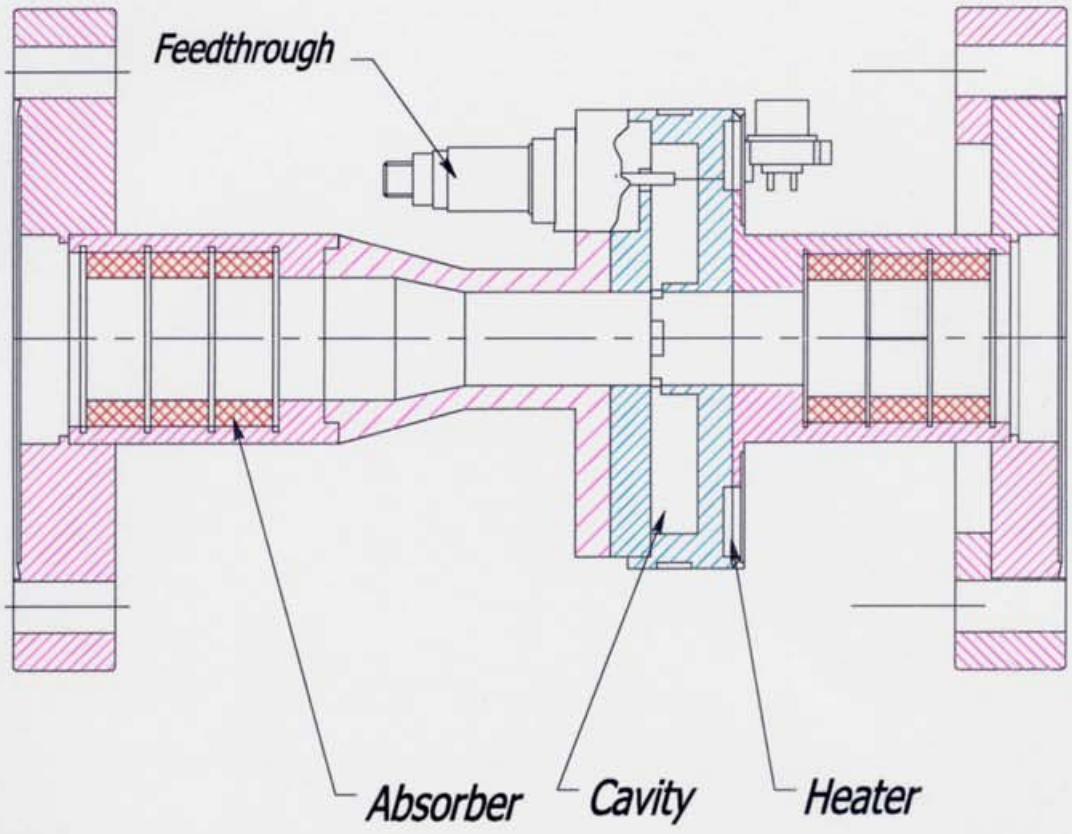


Figure 2-17: Phase sensor geometry.

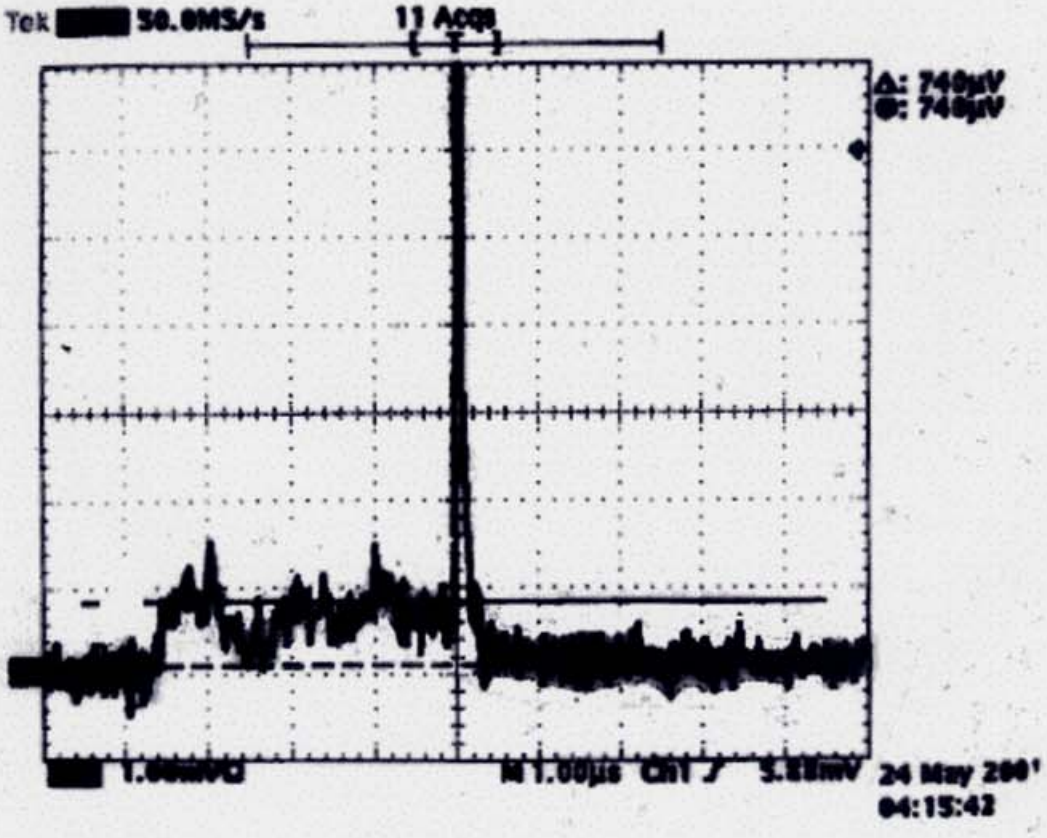


Figure 2-18: Output diode voltage from the phase sensor (old design)

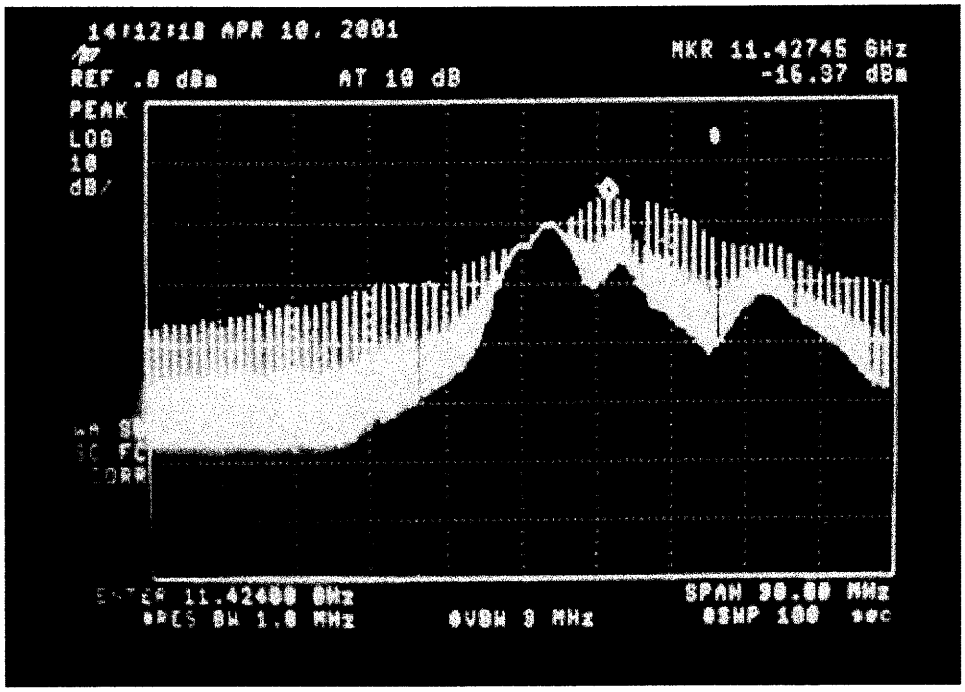


Figure 2-19: Spectrum from phase sensor (old design).

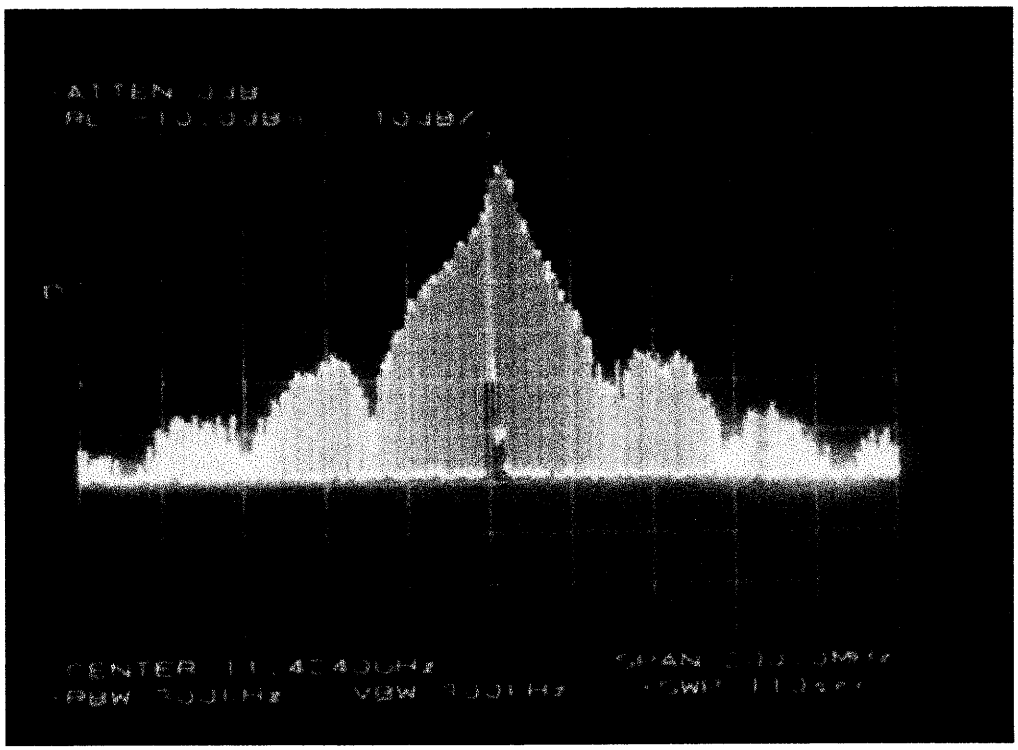

Figure 2-20: Phase sensor spectrum (new design).

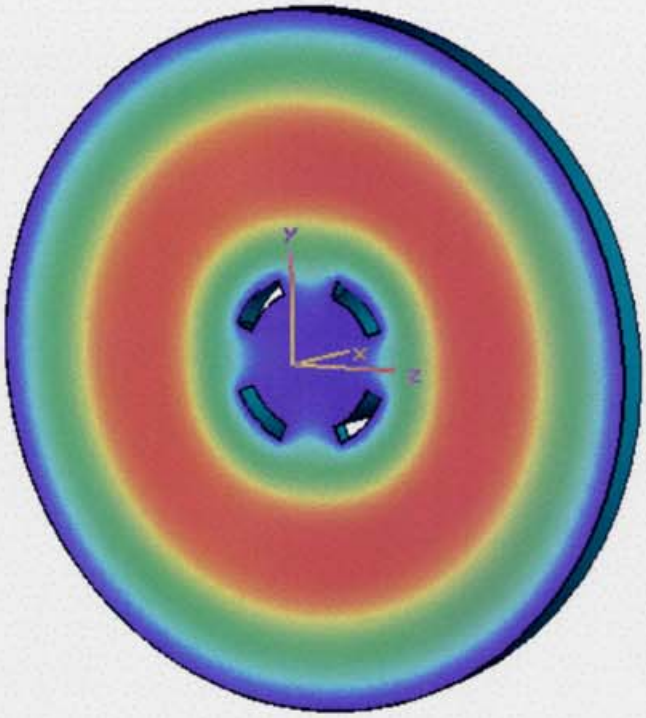

Figure 2-21: Electric field in the phase sensor mode TM010, frequency 5,712 MHz.

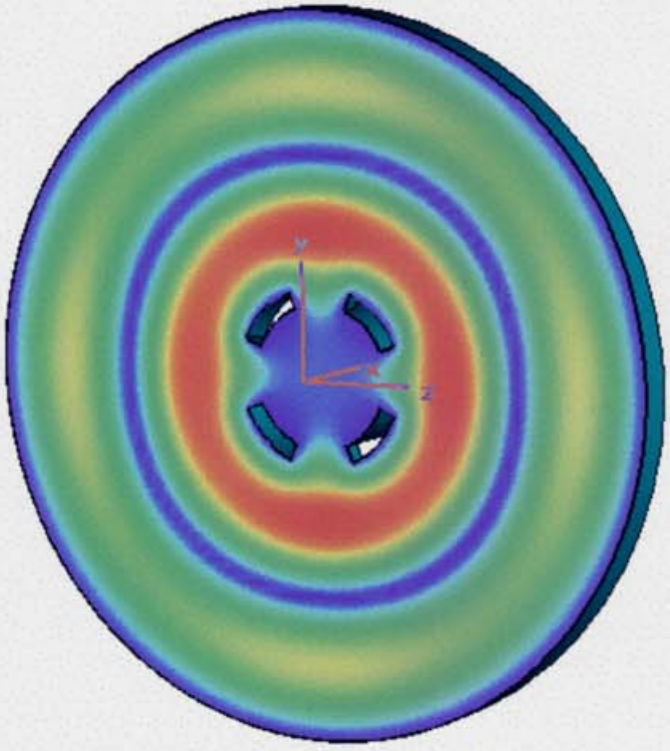

Figure 2-22: Electric field view in phase sensor mode TM020, frequency 11,424 MHz.

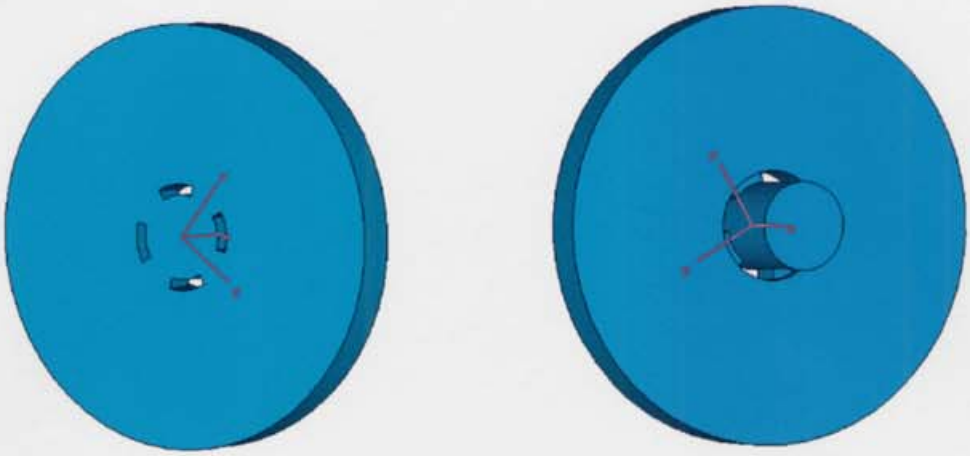

Figure 2-23:Model for phase sensor simulation.

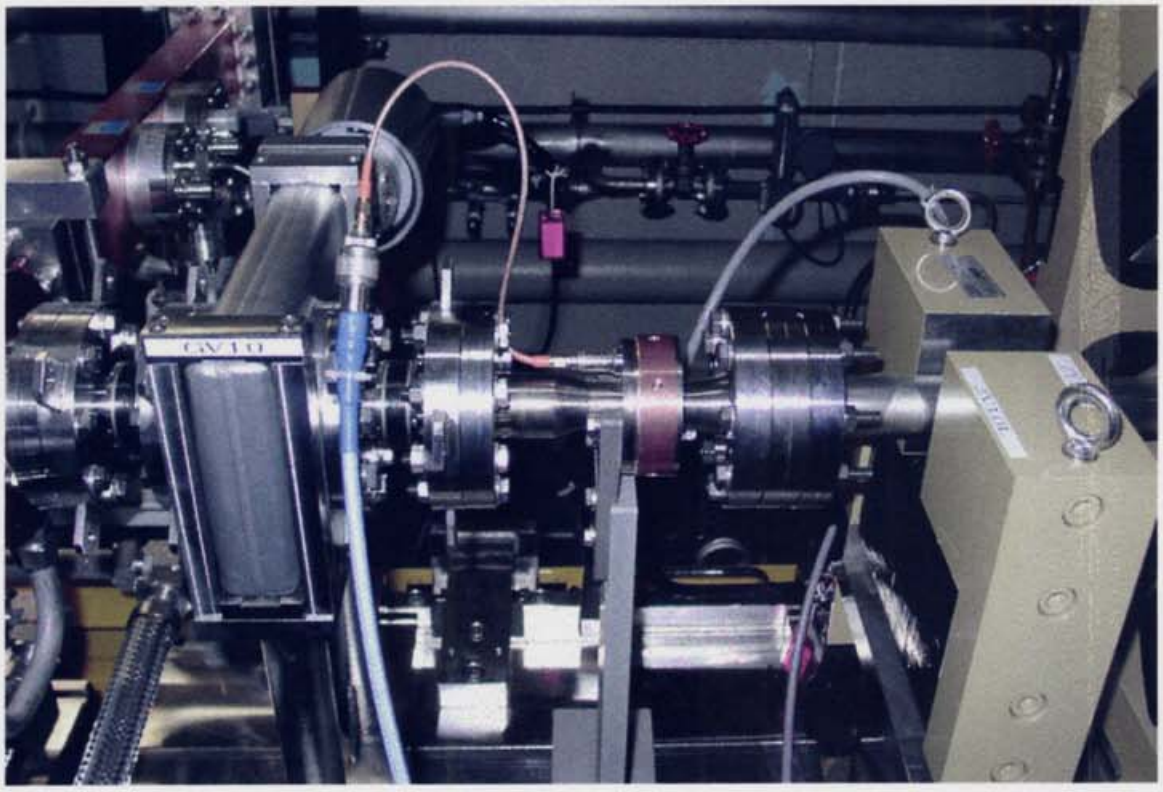

Figure 2-24: X- band phase cavity in the ATF KEK linac.

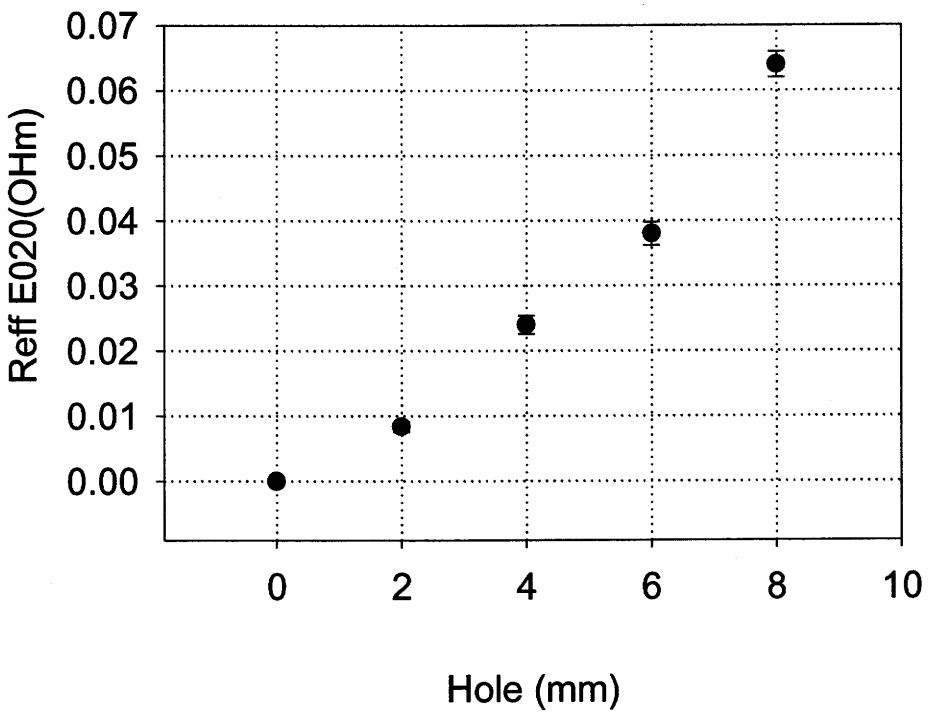


Figure 2-25: Phase sensor cavity impedances versus the beam pipe connection

slots.

Table 2-5: Parameters of the phase sensor.

| | |
|---|---|
| TM 010 frequency | 5,712MHz |
| TM0 20 frequency | 11,424MHz |
| Cavity radius | 34.55 mm |
| Cavity length | 16 mm |
| Beam hole radius | 8 mm |
| Q factor for TM020 | 2800 |
| Shunt impedance | 0.3 Ohm |
| Number of coupling slots | 4 |
| Slots width | 7 mm |
| Slots depth | 1 mm |

# Chapter 3

## Detection electronics design

## 3.1 Detection electronics for cavity beam position monitors

We can rewrite the expression, Eq. (2.25), for the output signal from the sensor cavity in terms of power, which is more useful for electronics circuits:

$$P_{out}(\delta) = \frac{\omega^2}{2Q} T^2(\sigma_z) M^2(h,\omega) \rho'(k\delta)^2 q^2 , \qquad (3.1)$$

where $q$ is the beam charge,

$M(h,\omega) = \sin(kh/2)/(kh/2)$ is the beam transit factor,

$T(\sigma) = \exp\left(-\frac{\omega^2\sigma^2}{2c^2}\right)$ is the beam length factor,

$\rho'$ is the normalized transverse shunt impedance,

$Q$ is the loaded quality factor,

$\omega$ is the cavity circular frequency,

$\sigma_z$ is the bunch length, $h$ is the cavity length, $c$ is the light speed, and $k$ is the wave number.

For our cavity sensor and the ATF beam charge, we need the electronic sensitivity of 5*10E-11 Watts for the beam position resolution of 0.2 microns. Another requirement for electronics is the output of phase, because the phase of oscillation in the cavity depends on the beam offset relative the cavity axis.

Figure 3-1 shows a simplified diagram of the cavity RF BPM electronics. When a bunched beam passes through the BPM cavity and if it has an offset relative to the cavity axis, it excites the TM110 mode, whose amplitude is proportional to the beam displacement $\delta$, the beam charge $q$ and depends on the beam length $\sigma_z$. The sign of the phase depends on which side of the cavity (left or right, top or bottom) the beam passes through. In the reference cavity, a beam excites symmetrical modes TM010 and TM020, whose amplitudes are proportional to the beam charge. The output voltage for TM020 mode has same dependence on the bunch length as the sensor cavity because its frequency is the same.

The output signal for the TM020 and TM010 modes do not depend on the beam position. To measure the amplitude and the sign of the phase from the cavity BPM, we propose to use the two-stage synchronous detection circuit.

First, the signals from the sensor cavity and the reference cavity go through band-pass filters to the first mixer where they are mixed with 5,712 MHz continuous signal. Then they go to the synchronous detector where the position signal is rectified. The signals after the circuit have the amplitude which depends on the beam position and the sign of the phase which depends on the sign of the beam offset in the cavity. To ensure the linearity in the mixer, the amplitude level of the phase reference signal is kept constant by the limiting amplifier. After limiting amplifier, the reference signal goes through the phase adjuster to maximize the position signal to the synchronous detector.

To protect the input circuits for the case of big beam offset, we install electrically controlled attenuator after band-pass filter, which is also used to change the BPM resolution. For our cavity, the maximum offset of the beam from the center axis can be 9 mm and it can produce about 20 W powers to electronics. On the other hand, the thermal noise, which is one of reasons to limiting the electronics resolution, is about 5*10E-13 W. It is clear that it is impossible to cover such large dynamic range. The dynamic range of our electronics is about 56dB. Attenuators can add 20dB.

More details about the circuit are showed in Fig. 3-2. This circuit is built to work with five cavity sensors and one reference cavity. It can measure both the X and Y positions of the beam. The outputs from TM010 and TM020 modes are used as the beam charge and the beam length sensors. The behavior of power after the limiting amplifier is showed in Fig. 3-3. The typical shapes of the signal after limiting amplifier are shown in Fig. 3-4.

We decided to use two outputs for beam position measurements. The one signal is the output from the logarithmic amplifier, and it is used to measure the beam offset when it is big. The dynamic range of this output is about 70 dB, and we can measure the beam offset up to a few mm. Another signal is the output from the synchronous detector. This signal is used for a small or normal beam offset.

The output amplitudes from the logarithmic amplifier and the synchronous detector are plotted as functions of the input power in Figs. 3-5 and 3-6, respectively. The typical shape of the output signals in the oscilloscope from the both detectors is shown in Fig. 3-7. Note that amplitude in the output from the logarithmic amplifier is linearly proportional to the beam offset in the both directions. This signal, however, does not give us the information on the sign of the beam offset.

## 3-2 Summary

We develop simple, low cost detection electronics for the cavity BPM system working at frequency of 6,426 MHz. The sensitivity of this electronic was measured to be better than 5*10-11 W.

To measure the amplitude and the sign of the phase from the cavity BPM, we propose to use two-stage synchronous detection circuits. To increase the dynamic range of our electronics, we proposed to use two output signals. The signal from the logarithmic output has a big dynamic range and low resolution, while the signal from synchronous detector has good resolution but does not have a big dynamic range.

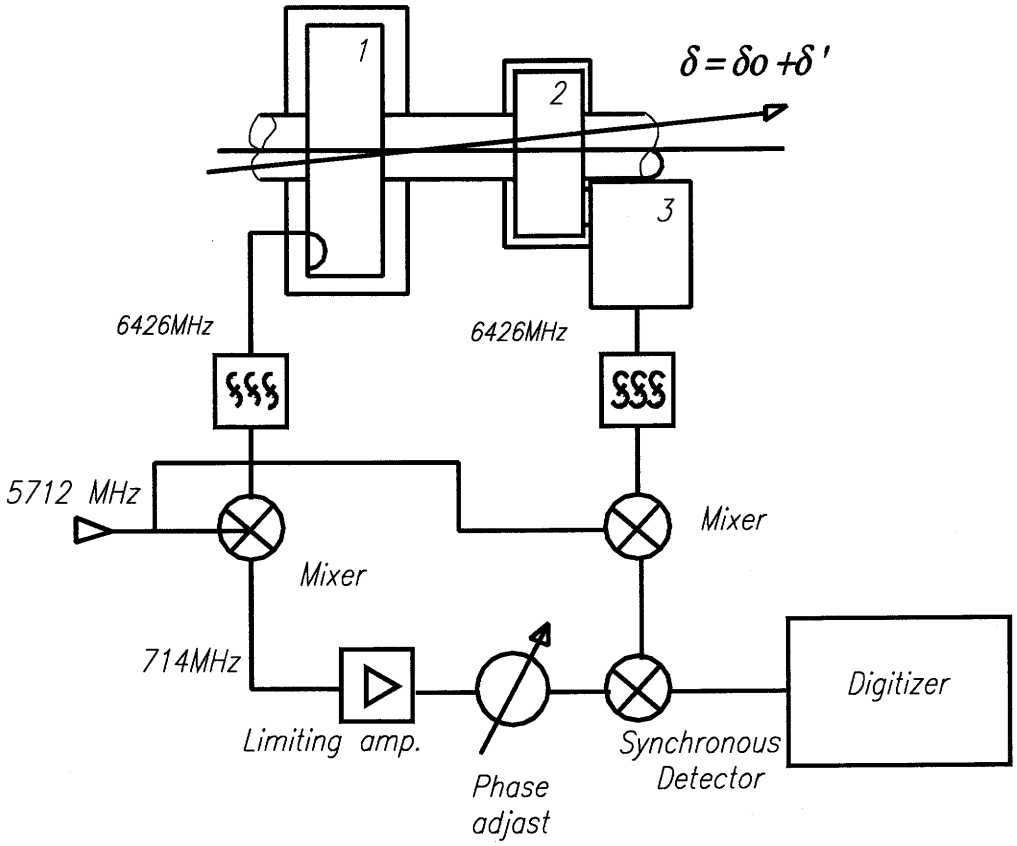


Figure 3-1: Diagram of the RF detection electronic for the cavity BPM
1 – Reference phase sensor, 2 – Position sensor cavity,
3 – Cavity sensor waveguide output.

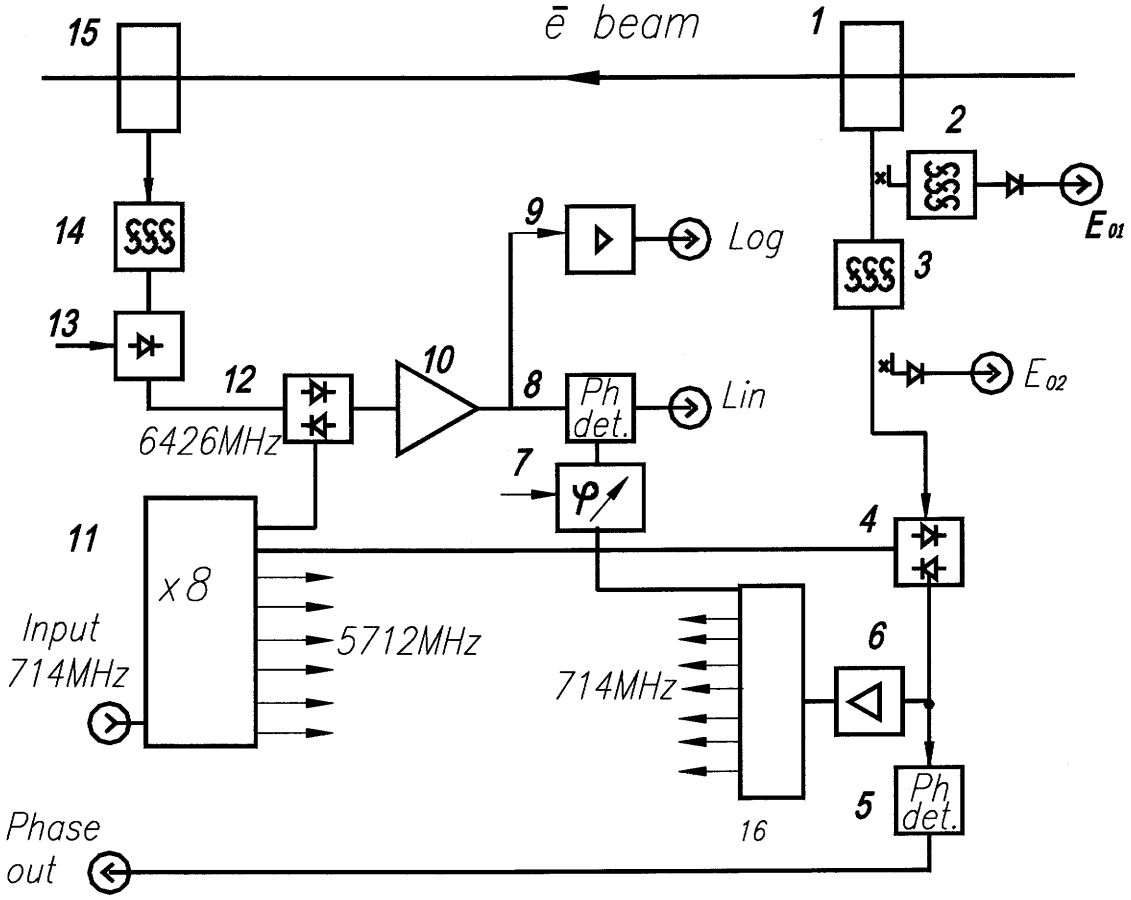


Figure 3-2: RF processing electronics diagram

1 – Reference cavity.
2 – Band pass filter 2,856MHz.
3, 14 – Band-pass filter 6,426 MHz.
4, 12 – Mixer 5,712MHz and 6,426MHz.
5 – Synchronous detector for measurement of the damping ring beam phase to the extraction line beam phase.
6 Limiting amplifier.
7 – Phase adjust for each measuring channel.
8 – Synchronous detector 714 MHz for beam position.
9 – Logarithmic amplifier.
10 – 714 MHz Amplifier 25 dB.
11 – Frequency multiplier and divider 714*8=5,712MHz.
13 – Attenuator.
15 – One of sensor cavity.
16 – 714 MHz 8 channel divider.

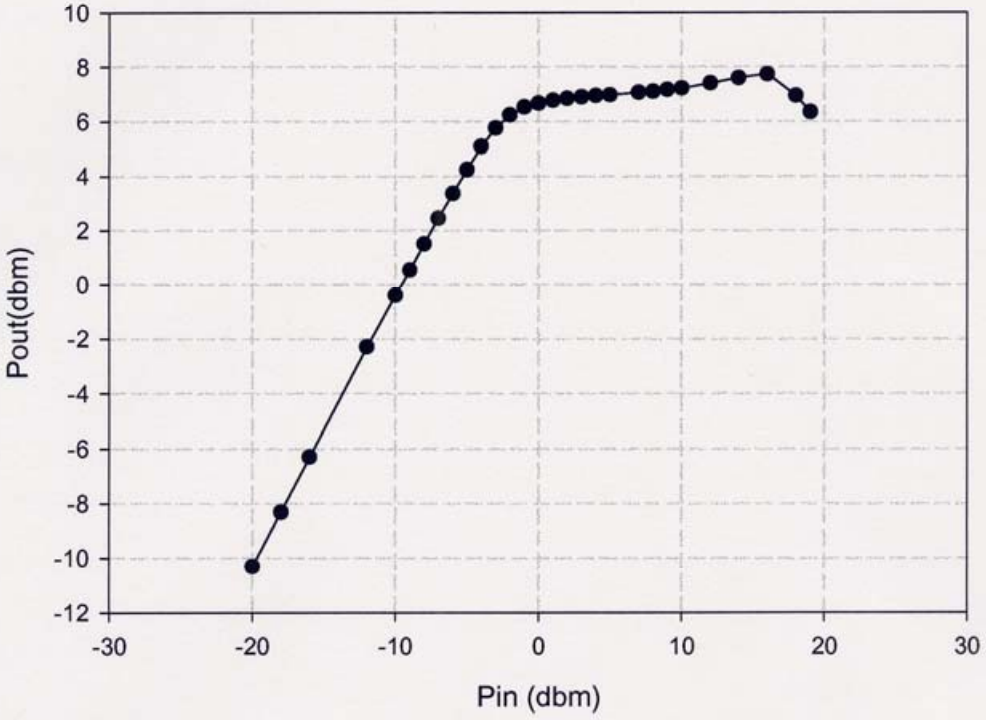


Figure 3-3: Power at the output of the limiting amplifier versus the input power

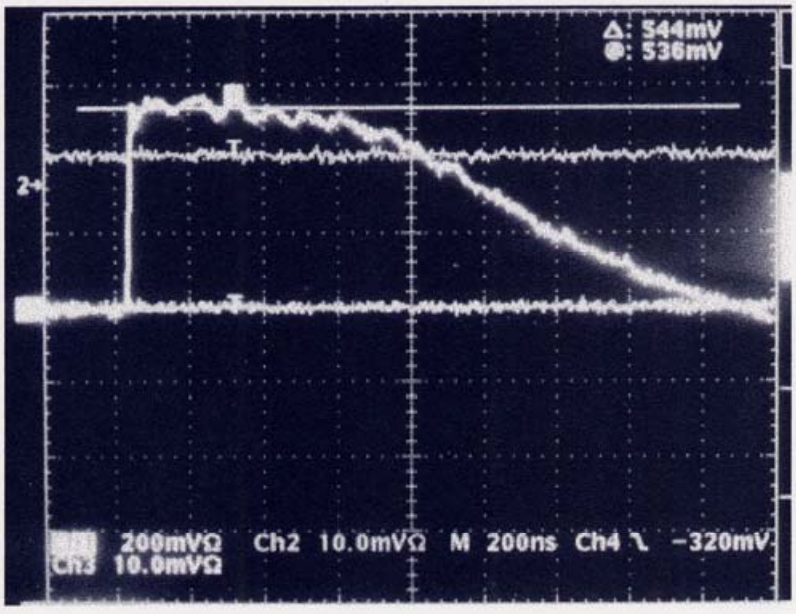


Figure 3-4: Pulse shape after limiting amplifier.

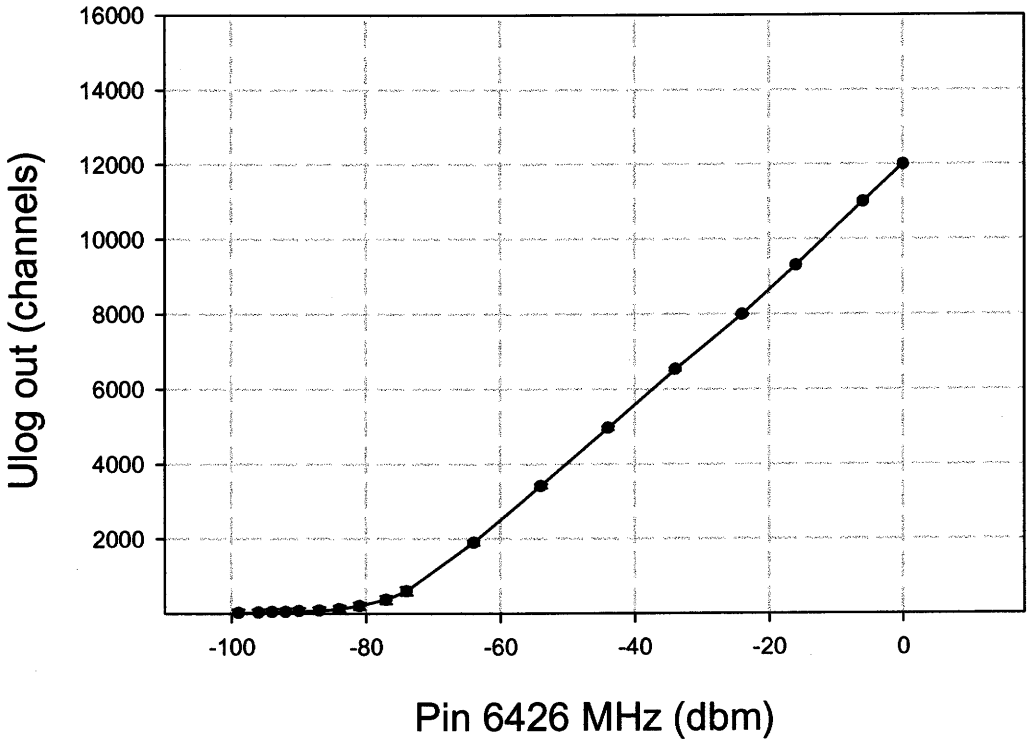


Figure 3-5: Output amplitude from the logarithmic amplifier versus the input power.

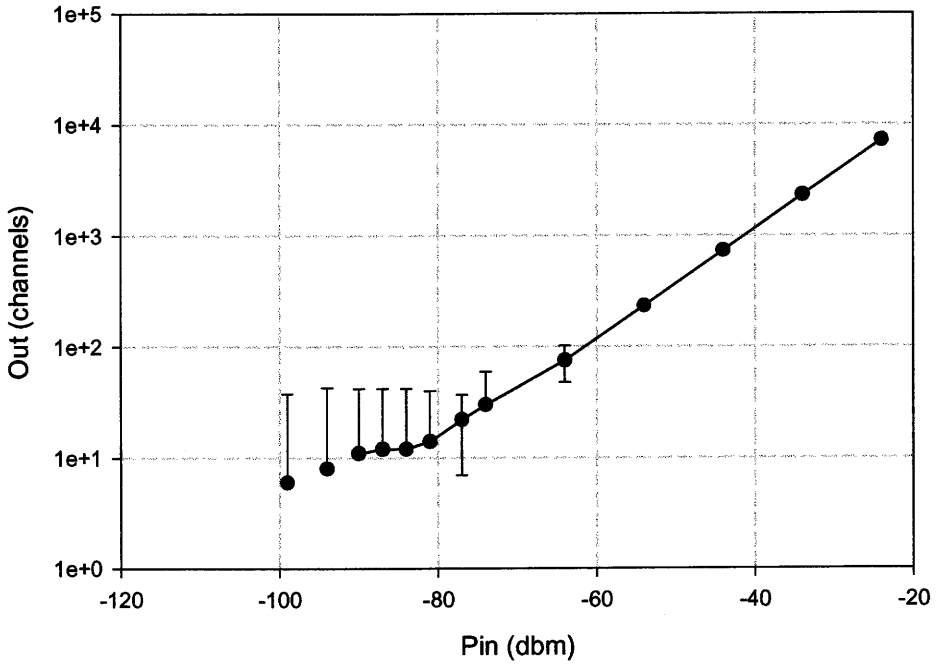


Figure 3-6: Output amplitude from the synchronous detector versus the input power.

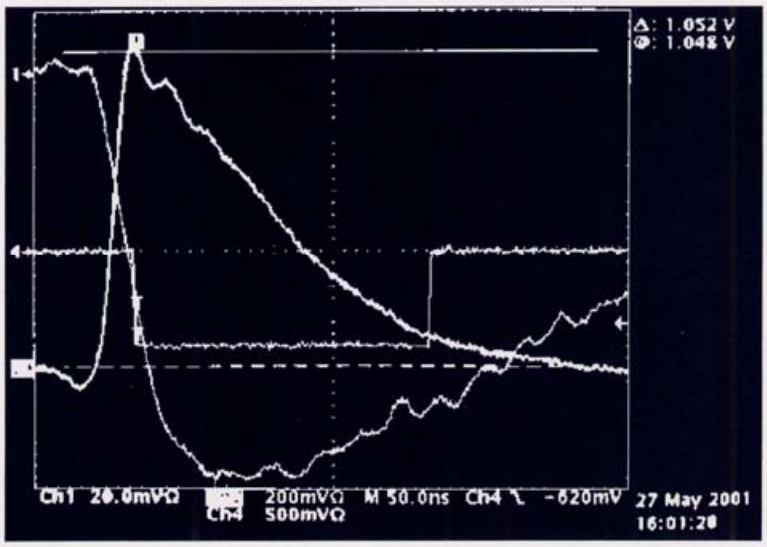


Figure 3-7: Shape of the output signals.
1 – Logarithmic amplifier output
2 – Synchronous detector output
3 – Strobe signal.

# Chapter 4

## Experimental results

## 4-1 Configuration and specification

In order to demonstrate high performance of the RF cavity BPM, three cavity BPMs and one reference cavity were installed at the ATF extraction line as shown in Fig. 4-1. The distance between the cavities is 190 mm. At the ATF, the beam has jitter as shown in Fig. 4-2. The beam trajectory, the beam length, the beam angle, and the beam population slightly vary from a bunch to bunch. By using those three BPMs, the measurement can be free from these jitter effects.

The measuring electronics are mounted on the NIM rack near the BPM setup as shown in Fig. 4-3. They are connected to the cavity sensors, (see Fig. 4-4) and the reference cavity (see Fig. 4-5) via RF cables. The digitizer electronics (14 bit ADC) were installed in the CAMAC rack located outside of the shielded area and are connected to the RF electronics through coaxial cables.

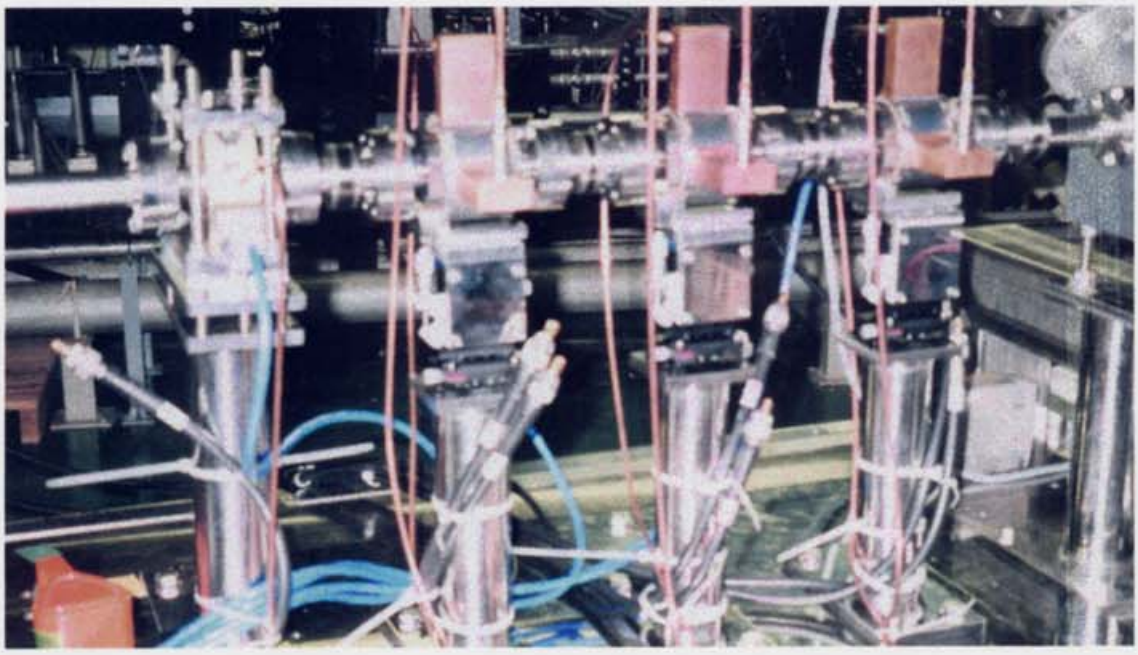

Figure 4-1: Three sensor and one reference cavity setup at the KEK ATF extraction line.

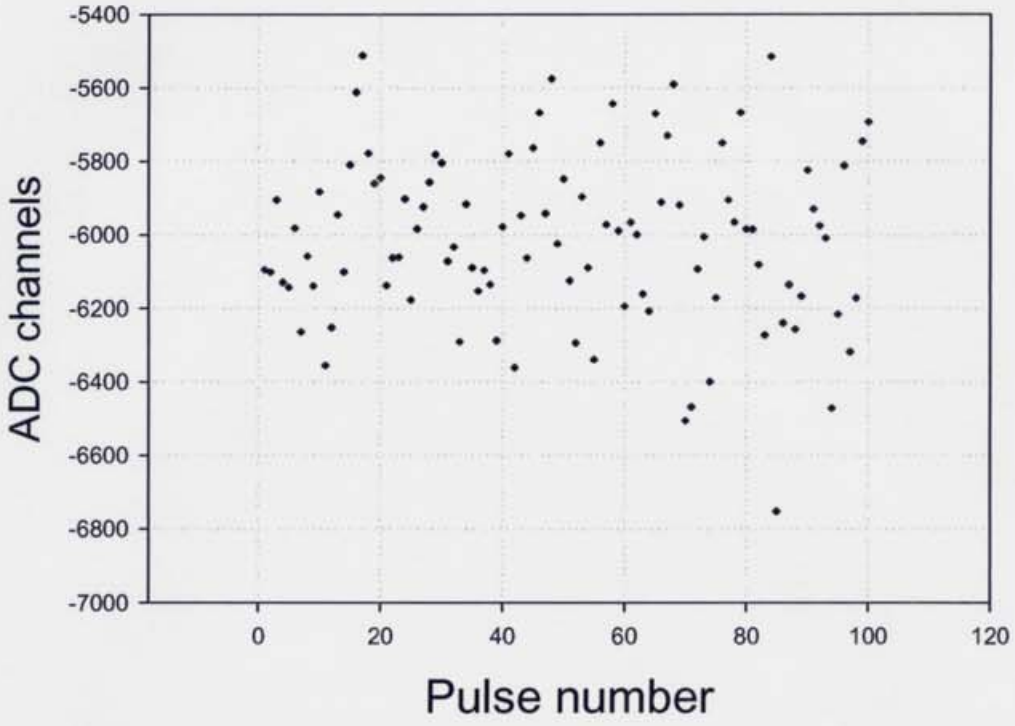


Figure 4-2: Output from one of BPM channel under the natural condition of the

beam position and charge jitters.

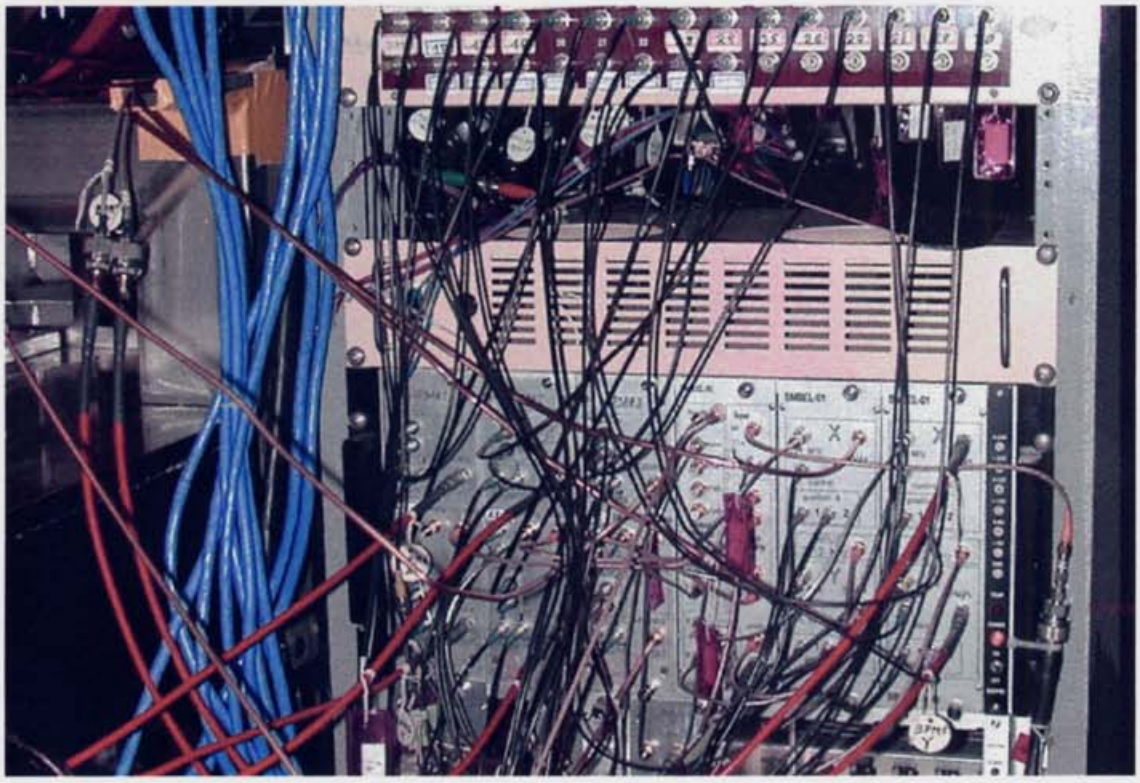

Figure 4-3: The measuring electronics for the cavity BPMs.

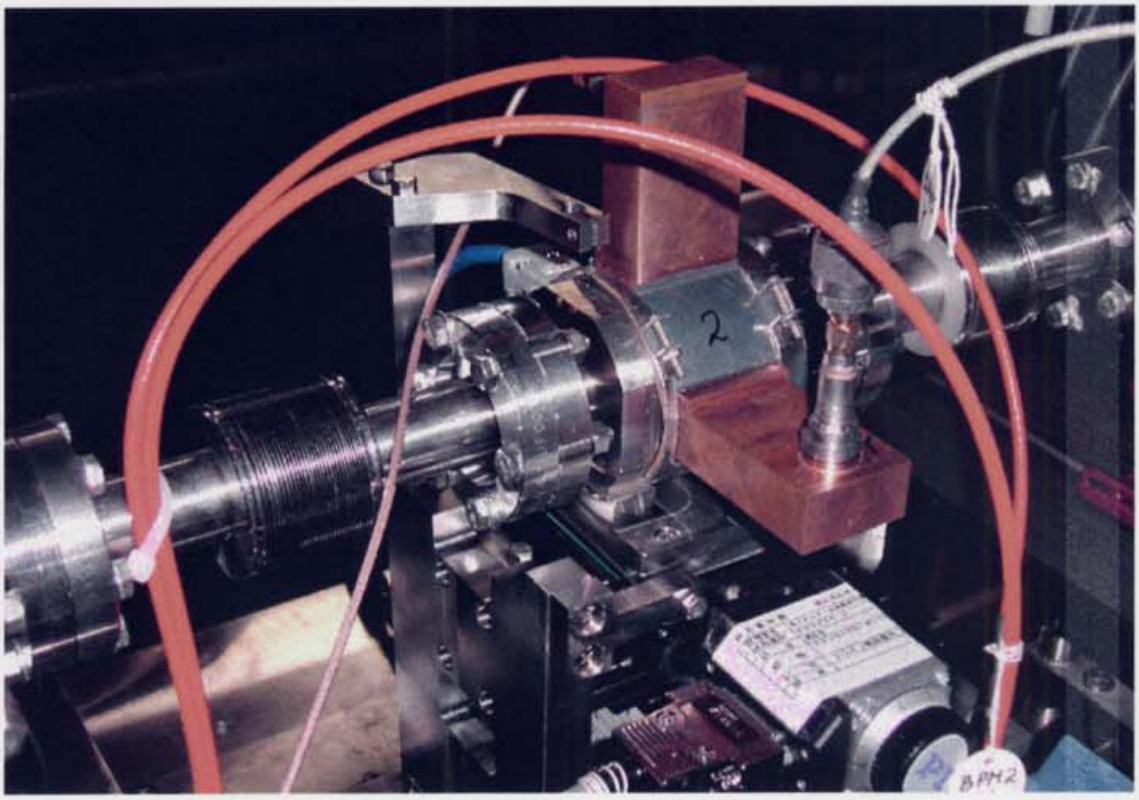


Figure 4-4: One of the cavity sensors at the KEK ATF extraction line.

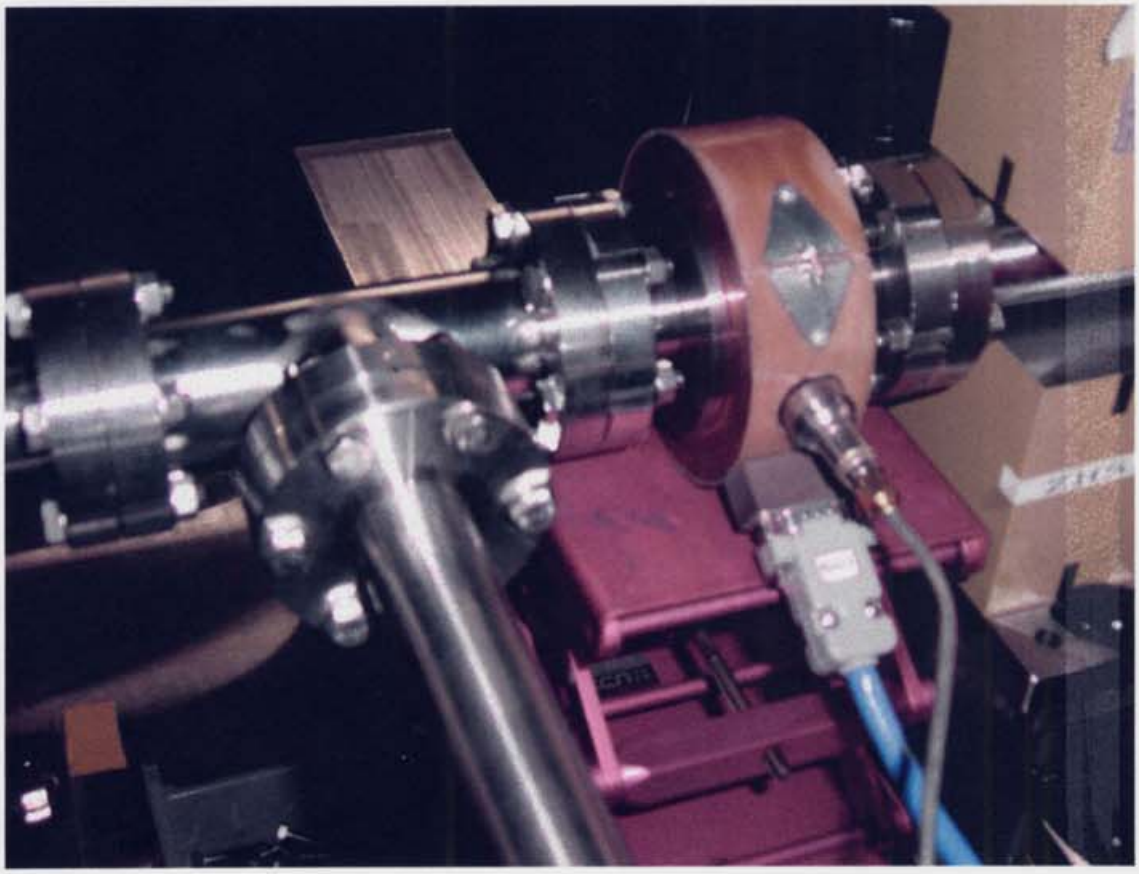

Figure 4-5: Reference cavity at the KEK ATF extraction line setup.

## 4-2 Data analysis

The resolution of the BPMs was measured using the triplet stack. In the triplet setup, the three BPMs are equally spaced. If the beam trajectory can be approximated as a straight line going through them, the beam position obtained at the middle BPM should be equal to the average of the positions obtained at the BPMs of both sides. If all BPMs of the of triplet have the same resolution and if the measuring electronics have uncorrelated noise, the resolution of the BPMs can be calculated from the standard deviation of the difference between the position at the center BPM and the positions averaged between the two surrounding BPMs over many beam trajectories [10]. The formula is given by

$$\sigma_{cbpm} = \sqrt{0.67}\sigma_{(1+3)/2}\ , \qquad (4.1)$$

where $\sigma_{cbpm}$ is the average standard deviation of the BPM position resolution and $\sigma_{(1+3)/2}$ is the standard deviation of the beam position difference between the signal from the central BPM and the signal averaged over the surrounding two BPMs.

Because our setup has no mover for BPMs, the calibration of sensitivity was done by using data from the ATF bottom BPMs located near our triplet setup. To steer the beam trajectory to the center of BPMs, we used the steering coils. Most of the data for resolution analysis were taken under the natural beam position jitter in the ATF extraction line. Figure 4-6 shows the best set of the experimental data, where the vertical axis is the beam position data from the middle BPM, and the horizontal axis is the beam position obtained by averaging the position data from the surrounding two BPM. All data were normalized to the same beam charge and bunch length using data from the reference cavity.

Then, we moved the beam trajectory many times using one of steering coils. Figure 4-7 shows the distribution of the difference between the two position data at the center BPM show in Fig. 4-6. Using the Gaussian fit, we found the standard deviation to be 217 mm. This gives us from Eq. (4.1) a BPM resolution of 177 nm for a single bunch with number of particle of 4 ~ 8*E9. The dynamic range of position measurement depends from electronics dynamic range and in these high resolution cases it is about 250 micron. Figure 4-8 shows the correlation of amplitudes between the output from the reference cavity at high frequency (6,426 MHz) and at low frequency (2,856 MHz) for three different RF voltages in the accelerating cavity in the ATF damping ring. Due to the bunch charge jitter, the data are scattered on straight lines.

This figure demonstrates that the reference cavity BPM can be used for bunch length measurements.

## 4-3. Experimental result for the bunch angle measurement.

Even when the beam passes exactly through the cavity center, it can excite the TM110 mode due to non-zero trajectory angles. This voltage becomes 90 degree out-of-phase from the beam current. In this case, the beam can also excite the voltage at TE110 mode. For our sensor cavity, this frequency is 8,750 MHz.

The output signal of this mode will be attenuated in the input band–pass filter to about -50db. But it is likely due to the limiting value of cavity $Q$ factor and the wide-band spectrum of the short bunch that the part of power of this mode can go through the filter. The power attenuation for this mode can be written as:

$$R = 10\log(Q_{11}(1-\omega_{TM11}^2/\omega_{TE11}^2)), \quad (4.2)$$

and it is about -35db for our case.

The plot in Fig. 4-9 shows the output signal from the cavity BPM versus the beam trajectory angle. In this experiment, the phase in the measuring electronics for one of BPM channel was moved out-of-phase to 90 degrees. In this case, this channel can not measure the beam offset. It can only measure signals that are in quadrature with the beam position signal. The beam trajectory was adjusted by the steering magnets at the extraction line. The beam angle measurement was done by ATF BPMs. It is not so clear now which of above two mechanisms is responsible for this behavior. It needs additional study.

## 4-4. Summary.

The RF cavity BPM system was designed. We installed five cavity sensors and one reference cavity to the KEK ATF extraction line. From the three-cavity and one reference cavity setup, we measured the position resolution of the cavity sensor to be 177nm. The measurement confirmed the calculation. The resolution is better than our goal, but this is not limitation for this type of position sensor. The resolution can be improved by changing electronics circuits. The measured beam angle resolution was about 5 μrad.

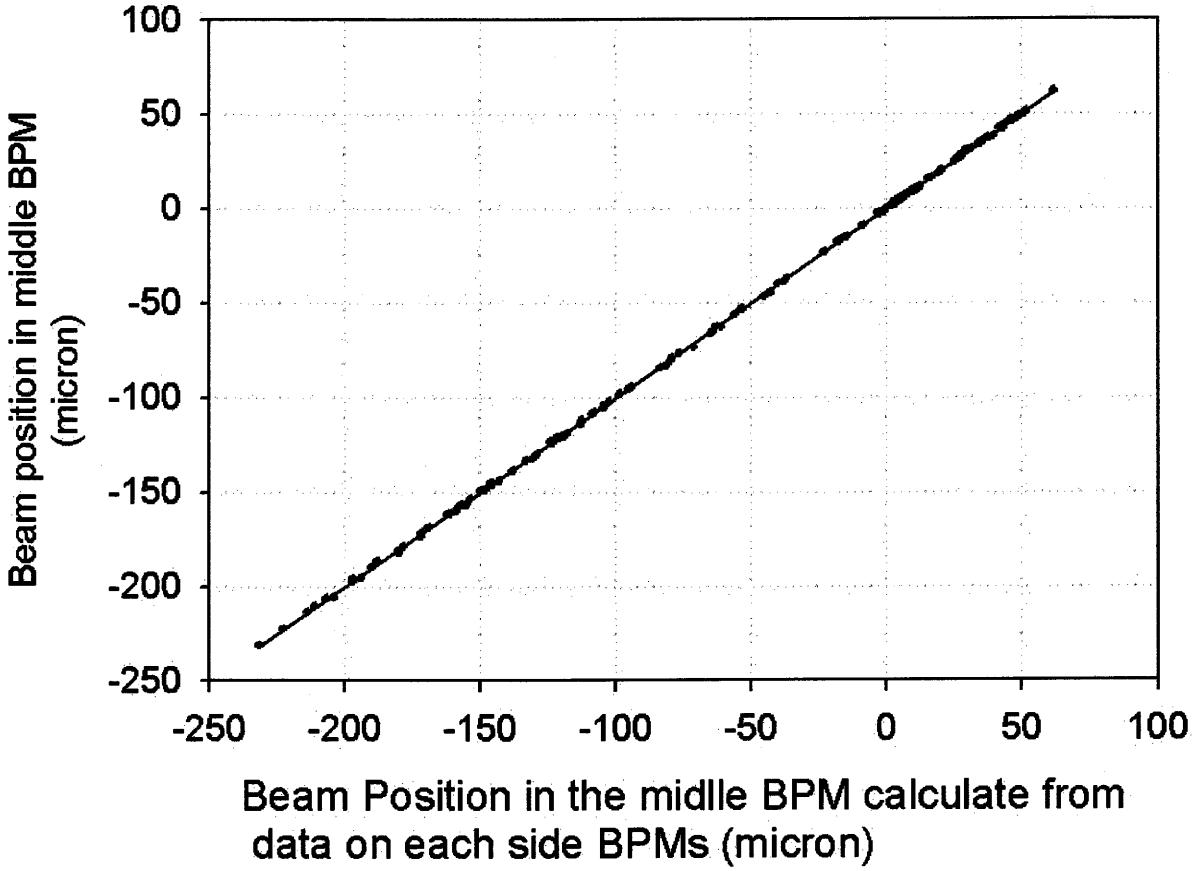


Figure 4-6: Correlation between the position data at the middle BPM and averaged one over the two surrounding BPMs.

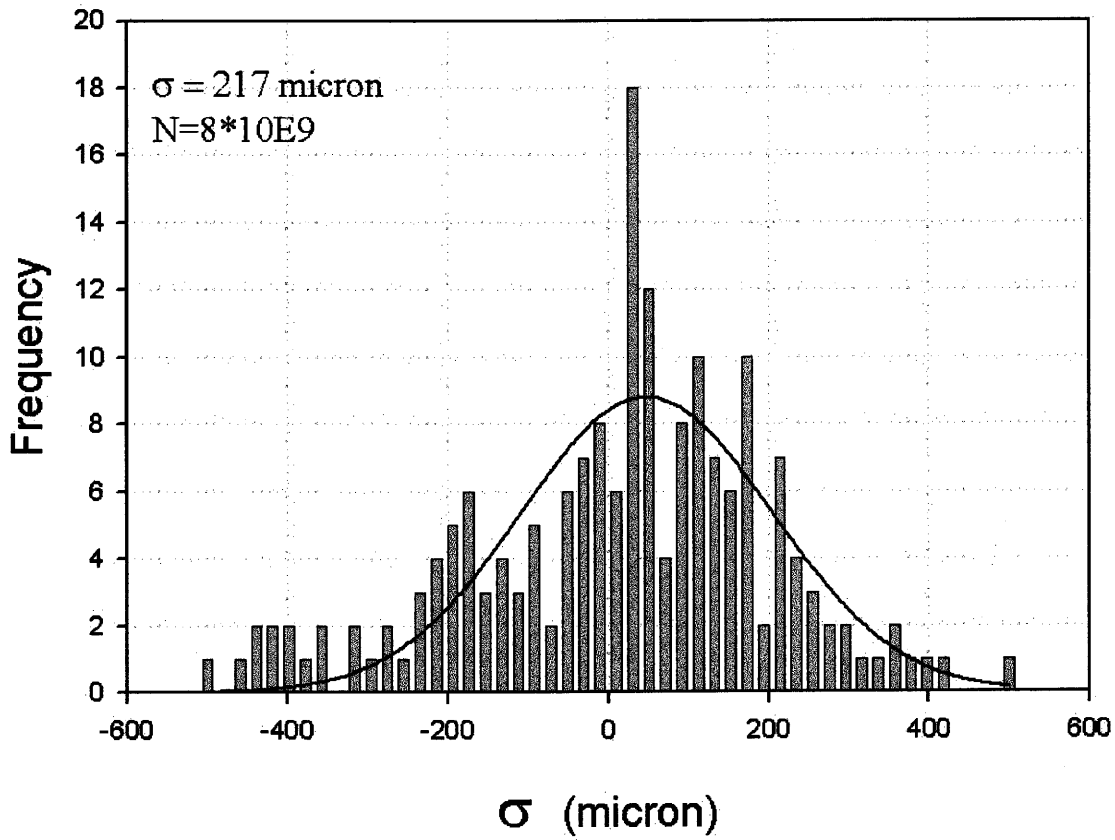


Figure 4-7: Distribution of the difference between the two position data and Gaussian fit.

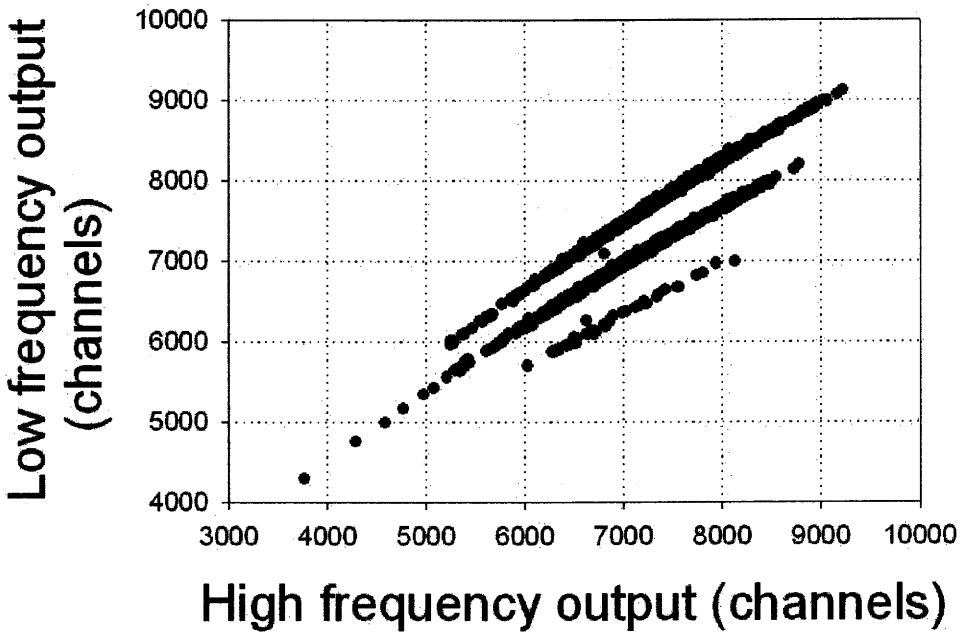


Figure 4-8: Output from the reference cavity. Three lines corresponded to deferent voltages at the accelerate cavity in the damping ring.
Data were taken in natural charge jitter condition in ATF.

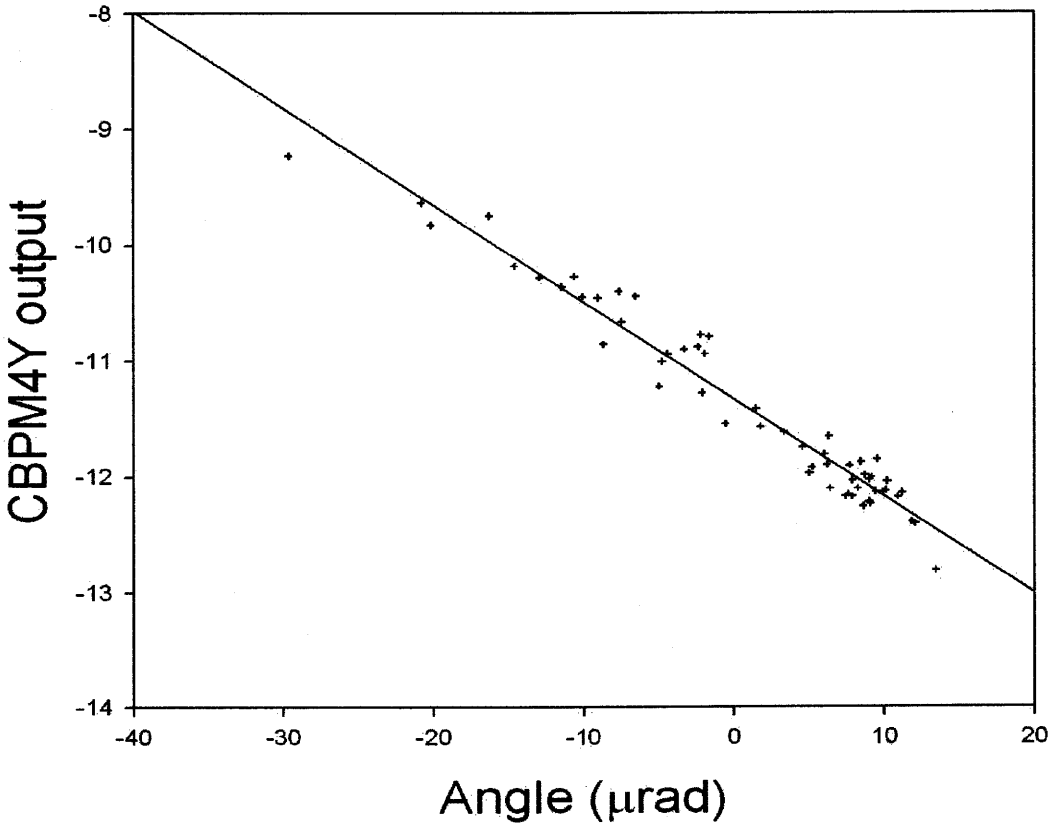


Figure 4-9: Cavity BPM signal versus the beam trajectory angle.

# Chapter 5

## Conclusions and summary

Future linear colliders such as JLC/NLC demand a very high resolution BPMs (less than one micron) for measurements of the beam position. The position sensor which has a high accuracy to satisfy this requirement needs to be developed. The RF cavity is one of the best candidates for this kind of task. The basic idea of the cavity RF BPM was proposed in 1960's. In early 1990's ,VLEPP group has proposed a microwave BPM system to measure a very small beam displacement in nm range for the single-bunch operation [3].

In 1998, the T. Sintake group installed a BPM system with three C-band cavities to the SLAC FFTB and achieved resolution of 25 nm for a beam with 1nC charge [11].

At 1998, the BINP group achieved 150 nm resolutions at the BNL ATF experiment using 14 GHz cavities [7]. In 1999, the KEK ATF group decided to use the cavity BPMs to measure kicker jitters and to use precise beam position data from these BPMs to calculate the emittances. The work presented in this thesis is a part of this activity. The achievements and findings of this work can be summarized as follows:

(1) We have designed and built the cavity BPMs system, which consists of five sensor cavities operated at 6,426 MHz and one reference cavity whose one of operating mode has the same frequency as the sensor cavities. To calibrate the output signal of the beam position for different bunch charge and bunch length, we used additional output from the reference cavity at 2,856 MHz. The cavity BPM system can be used in both the single- and multi-bunch operational modes.

(2) From the triplet setup using three BPMs and one reference cavity, it was fonded that the resolution is better than 200 nm. The real resolution of the BPMs may be even better than the achieved one, since the experimental constraints such as lack of position movers prevented us to install all BPMs exactly in the line with the beam trajectory.

(3) The dynamic range of the position sensors for the horizontal and vertical directions was measured to be 54 dB.

To protect the measuring electronics from big signals coming from beams with large position offset, as well as to enhance the dynamic range, the electrically controlled attenuators were installed after the output of all cavities.

(4) The RF cavity BPM system is now an important part of the main beam measurement and diagnostic system in the KEK ATF extraction line. The KEK ATF is first accelerator in the word where the RF cavity BPMs systems are included in the main beam diagnostic equipments.

(5) The phase feedback system for LC was proposed. For this system, the new type of X-band oversized two-mode phase sensor was proposal, designed and installed to the ATF linac. The performance of X-band phase sensor was measured at the KEK ATF linac.

# Acknowledgments

I would like to acknowledge the suggestion of the RF cavity BPM problems to the Prof. Vladimir Balakin.

I would like to thank Prof. Hitoshi Hayano for his help in the BPM installation at the KEK ATF and assistance in the BPM resolution experiment. Without him this work would not have been successful.

I wish to thank Profs. Koji Takata and Yong Ho Chin for their big help and interest in this work.

I wish to thank Mr. Anatolij Bazhan, Mr. Pavel Lunev, Dr. Nikolay Solyak and Mr. Pavel Zhogolev for the assistance in the ATF BNL/KEK experiments and for their helpful suggestions and comments.

I wish to thank the BINP Protvino group for manufacturing of the cavities and specially Mr. Dmitry Valyaev and Mr. Ury Savinok for the electronics turning.

# References

[1] International Study Group Progress Report, KEK Report 2000-7, April (2000).

[2] W.Schnell "Common-mode rejection in resonant microwave position monitors for linear colliders" CERN-LEP-RF/88-41, CLIC Note 70.

[3] V. Balakin, V.Vogel, N. Solyak, "The model of Beam Position Monitor for VLEPP", Proc. Third International Workshop on Linear Colliders, v. 3, p. 188 (1991).Protvino.

[4] V. Balakin, A. Bazhan,..V.Vogel et al., "Beam Position Monitor with nanometer resolution for Linear Collider", Proc. Fourth European Particle Accelerator Conference, v. 2, p. 1539 (1994).

[5] V. Vogel " Beam position monitor with the nanometer resolution for VLEPP" , Proc of Emittance'93, Apr. 1993, Tsukuba.

[6] T. Shintake, "Experimental Results from FFTB December 1995 run", Brief Memo (1996).

[7] V.Balakin, .. V.Vogel at al., Experimental Results from a Microwave Cavity Beam Position Monitor ". Proc. Of the 1999 PAC, New York, 1999

[8] J. P. H. Sladen, I. Wilson, W. Wuensch, "CLIC Beam Position Monitor Tests", CERN-LEP-RF (1996).

[9] N. Zinevich, A. Filipov "High resolution BPM for Linear Collider" Preprint 89, BINP, Novosibirsk (1988). (In Russian).

[10] R. Assmann, B. Dehning, J. Matheson "Use of Movable beam position monitors for beam size measurements" Proc. EPAC 2000, p.1693. (2000).

[11] T. Shintake "Development of Nanometer Resolution RF-BPMs", Proc HEACC'98, Dubna, Russia (1998).

[12] M. Tejima et al., Proc. LINAC'94, Vol. 2, pp.914-916, (1994)

[13] H. Hayano,T. Shintake "Submicron Beam Position Monitors for Japan Linear Collider" KEK Preprint 92-118, (1992)

[14] I. Yoshida, H. Hayano "Development of high resolution multi-bunch BPM" Proc. Of 24th Linear Accelerator Meeting in Japan, Sapporo, p.371, (1999)

[15] R.B.Neal, "The Stanford Two-mile Accelerator" Inc., New York (1968)

[16] G. E. Fisher, CLIC Note 63, May (1988)

[17] V.Teryaev, "The possibility of measurement of bunch length by using pillbox cavity" BINP Preprint, 2001. (In Russian).

[18] J.Frisch, D.McCormick, M. Ross, " Tilt Monitor and Nanometer Resolution BPM Studies"

[19] R. Lorenz, K Yezza, "Test Results on Beam Position Monitor Prototype for the TTF", Proc. Fourth European Particle Accelerator Conference, v. 2, p. 1536 (1994).

[20] O.Milovanov, N.Sobenin "Tecknika sverhvysokih chastot", Atomizdat, 1980. (In Russian).